EUROPEAN ORGANIZATION FOR NUCLEAR RESEARCH

CERN / SPSC 2003–001
SPSC / M693
January 7, 2003

MEMORANDUM

NA60 status report

The NA60 Collaboration

This memorandum reviews the status of the NA60 experiment, with emphasis on the progress made over the year 2002. It gives a brief account of some detector development issues and reports on the 2002 beam time periods and respective data analysis.

1 Introduction

1.1 Overview of the NA60 experiment

The NA60 Collaboration is presently composed of physicists from the following institutions: Bern, BNL, Cagliari, CERN, Clermont-Ferrand, Lisbon, Lyon, Palaiseau, RIKEN, Stony-Brook, Turin and Yerevan. The collaboration has proposed an experiment to study prompt dimuon and charm production with proton and heavy ion beams at the CERN SPS. The proposal [1] was approved by the Research Board in the year 2000, for a 2-week long commissioning run in October 2001, followed by physics runs in 2002 and 2003, with proton and ion beams.

The NA60 detector complements the muon spectrometer and zero degree calorimeter previously used in NA50 with new state-of-the-art silicon detectors, placed in the target region. A radiation hard beam tracker, based on a set of silicon microstrip detectors operated at 130 K, is placed on the beam line, upstream of the target system. It gives the transverse coordinates of the impact of the incident beam particles on the targets with a precision around 20 μm. This allows us to identify the interaction point with enough accuracy to measure the offset of the muon tracks, and thereby select events where a pair of D mesons was produced, even in the low multiplicity p-Be collisions.

Downstream of the target system, and inside a dipole magnetic field of 2.5 T, we have a silicon tracking telescope, that tracks the charged particles and allows us to identify which one of them provides the best match to the muon measured in the muon spectrometer, placed behind a 5.5 m long hadron absorber. For proton runs, this telescope is made of silicon microstrip planes complemented by pixel planes. For the ion runs, the very high multiplicity of charged particles imposes the exclusive use of silicon pixel detectors. We will have 16 pixel planes, 10 of 4 chips and 6 of 8 chips, made with 88 radiation tolerant ALICE1LHCB pixel readout chips [2], of around 8000 channels each.

Three test runs have taken place so far: two weeks in October 2001 and three weeks in June 2002, with proton beams, and 10 days in October 2002, with Pb ion beams of 30 and 20 GeV per nucleon. In 2003 the experiment will take data for dimuon physics studies with proton and indium beams.

1.2 Brief summary of the physics motivation

The studies of high energy nuclear collisions done at the AGS and at the SPS between 1986 and 2000 have established the boundary of confined hadronic matter, indicating a universal hadronization (Hagedorn) temperature, of around 150–180 MeV, whatever the energy of the colliding nuclei. These findings are in very good agreement with the predictions of statistical QCD, as obtained through lattice studies. In particular, there are strong indications that, above a certain critical value of the colliding nuclear mass or of the collision centrality, the partons produced in the initial stage of high

energy heavy-ion collisions at the SPS undergo a transition to a color condensate of interacting deconfined partons.

The detailed J/ψ suppression pattern determined using measurements of the NA38, NA50 and NA51 experiments, performed at the CERN SPS, seems to provide the first signal of such color deconfinement through parton condensation. However, even if the produced medium is not hadronic, it is not necessarily in a quark-gluon plasma phase. That would require that the color condensate medium live long enough to subsequently reach thermal equilibrium. No direct evidence has been observed, so far, signaling the presence of a thermalized partonic medium in the early stages of the nuclear collisions, when a QGP phase may form.

The NA60 experiment will measure the J/ψ suppression pattern in In-In collisions at 158 GeV/nucleon, to determine the critical scale for the onset of deconfined parton condensation. The comparison with the previously established suppression pattern, measured with Pb-Pb collisions at the same energy, should confirm the existence of suppression thresholds for the directly produced J/ψ's and for those originating from χ_c decays, and will provide a first study of the nuclear-dependence of these thresholds. NA60 will also look for the production of thermal dimuons, whose presence would indicate that the produced partonic state has existed long enough to reach equilibration, and will measure the yield of open charm mesons, the heaviest flavour that can be produced in nuclear collisions at the SPS energies and the natural normalization for the charmonia studies.

1.3 Sharing of responsibilities in the NA60 projects

This section lists the main projects of the NA60 experiment and the sharing of responsibilities for each project, among the members of the collaboration.

- The **Beam Tracker** detector is the result of a joint effort by several groups: Bern (read-out electronics), BNL (silicon sensors), CERN (assembly, integration), and Clermont-Ferrand (tests, operation). Most of the work is done under the coordination of Ernst Radermacher (detector assembly and integration) and Kurt Borer (electronics).
- The **Silicon Microstrip Telescope** was essentially built by the Lisbon and CERN groups, under the coordination of Carlos Lourenço (detector assembly) and Jan Buytaert (read-out electronics), with the participation of BNL (sensors) and of Stony-Brook (CCB cards).
- The **Silicon Pixel Telescope** is coordinated by Ernst Radermacher (detector assembly) and Gianluca Usai (read-out electronics), strongly involving the Cagliari, CERN and RIKEN groups.
- The setting-up and operation of the **Interaction Counter** is under the responsibility of Peter Sonderegger (Lisbon) and Jean-Yves Grossiord (Lyon). Bern provides the read-out electronics.
- The Turin group is responsible for the **Zero Degree Calorimeter** and for the **Quartz Blade** detector, under the coordination of Enrico Scomparin.

- The **Muon Spectrometer** and **Trigger** projects are coordinated by Jean Castor, Paul Force and Louis Kluberg, involving Cagliari (P2 and DAQ interfacing), Clermont-Ferrand (tracking chambers, trigger hodoscopes, RMH electronics, online monitoring) and Palaiseau (trigger electronics).
- The **Data Acquisition, Detector Control and Online Monitoring** Project is coordinated by Peter Rosinsky, involving the CERN and Lisbon groups. Most of the hardware interfaces between the front-end electronics and the DAQ system are taken care of by the Cagliari group.
- The **Offline Software** Project is coordinated by Ruben Shahoyan (Lisbon) with the participation of many institutes.
- The **Target** system was built in Yerevan and assembled at CERN.

1.4 Recent developments in the NA60 experiment

In the year 2002, the NA60 experiment had a first beam time period between May 27 and June 19, with a beam of 400 GeV protons. This beam time was primarily used to consolidate all the detector systems, including their readout electronics chains, as well as testing and debugging many improvements made to the DAQ and detector control systems. In the second part of the beam period the experiment could collect data for offline analysis.

Several new detector systems were tested and operated, essentially for the first time, in this beam period: the silicon microstrip telescope, the first 4-chip silicon pixel plane, and a new interaction counter. It was also the first time that the PT7 vertex dipole magnet was operated during long periods at the nominal current of 900 A. We faced two main difficulties: the PT7 magnet was abnormally heating and one of the two beam tracker stations did not properly work in the second part of the run. These two problems could not be solved before the end of the rather short beam period. Once the microstrip telescope was operational, we collected data with beam intensities between 2 and $5 \cdot 10^8$ protons per burst, on a target system made of In, Be and Pb targets. The interaction counter and the beam tracker information would not have been exploitable at higher beam intensities.

In October 2002, from 9 to 19, the experiment ran with a Pb ion beam of 30 and 20 GeV per nucleon, five days each. The vertex spectrometer was composed of the three 4-chip pixel planes that could be built by this time. Besides performing many detailed tests with these pixel planes, the run was also used to collect data for physics studies, debug the new initialization of the (old) system that selects the several kinds of trigger (dimuon, single muon, etc), and test a new procedure to measure the time delay between the two muons that give a dimuon trigger, using the P2 trigger hodoscope.

The full energy Pb ion run expected to take place in October 2002, after the low energy days, was cancelled. This was due to the fact that not enough silicon pixel planes could be assembled to track the hundreds of charged particles produced in such collisions. This loss of beam time in 2002 will be partially compensated by a

slightly longer run in 2003, but it is clear that, without our own Pb-Pb data, we will have to rely exclusively on the comparison with the NA50 data, with increased systematical uncertainties.

From the data collected in October 2002, and mostly as a demonstration of the performance of the silicon pixel telescope, we will be able to measure the charged particle multiplicities produced in Pb-Pb collisions, at 20 and 30 GeV per nucleon, and their pseudo-rapidity distributions, for several centrality bins determined by the ZDC energy.

In the following lines we describe in more detail the recent evolution of the NA60 detectors, data acquisition and detector control system. We will then report on the analysis of the data collected in 2002 and review the prospects for the 2003 runs, with proton and In beams, in terms of goals and foreseen performance.

This document is not intended to provide a complete description of the experiment but rather a complement to the proposal and other SPSC memoranda [3, 4]. In certain places, we have repeated previously provided information to improve clarity and ensure self-consistency.

2 The Cryogenic Beam Tracker

The cryogenic Beam Tracker, developed as a common project between the RD39 and NA60 collaborations [5], is a tracking telescope made of two stations of silicon microstrip detectors, positioned on the beam line just upstream of the target. It tracks the incident beam particles (protons or nuclei) and measures the transverse coordinates of the interaction point, at the target, with a position resolution of the order of 20 μm. It also provides a time stamp for each passing particle, with a timing accuracy of 1.7 ns. The two stations are placed at 10 and 30 cm upstream of the target centre, and make a 45° angle with respect to each other. Each station consists of two silicon microstrip sensors mounted back-to-back, on either side of a 6-layer printed circuit board, with the strips perpendicular to each other. The sensors are made of 24 strips of 50 μm pitch, surrounded by four wider strips on each side.

The detectors are placed in a vacuum box and run at 130 K to maximize the charge collection efficiency after collecting high radiation doses [6]. Their temperature is controlled by remotely setting the nitrogen flowing in the cooling pipes and by continuously adjusting the power dissipated by heaters placed on the PCB.

In the modules used for proton running, the strips are wire-bonded to a radiation-hard pre-amplifier chip specially developed to run at cryogenic temperatures. The modules used for ion runs are essentially identical, except that the front-end chip is replaced by a simple 'pitch-adapter' circuit, since the signals are large enough to be sent directly to the fast amplifier cards placed outside of the vacuum box. The amplified analog signals are then sent to the data acquisition system PC, placed in the counting room, through fast cabling and Multi-Hit Time Recorder (MHTR) FERA modules.

2.1 Operation in the June 2002 run

The proton beam tracker was tested on the beam for the first time during a few days in October 2001, with proton bunches every 25 ns. In spite of properly working during the previous laboratory tests, the detector performance was affected by pick-up noise during the operation in the beam line. This noise was caused by the CAEN switching power supplies and affected, through the cabling, the bias voltages provided to the detectors and preamplifier chips. For the June 2002 run this problem was eliminated by providing all the needed voltages through NIM modules built on purpose, equipped with noise filters and connected to each detector module by a shielded flat cable.

Four proton beam tracker modules were prepared for the June 2002 run, each pair mounted on a different cover of the vacuum box, so that we could replace them in only a few hours, keeping the cryostat and vacuum connections in place. The two modules of the first cover had already been irradiated in the October 2001 run and were operated during the first part of the June run, during the setting-up and debugging of all the NA60 detector systems. Both modules worked well and helped steering the beam through the beam hole of the microstrip and pixel silicon planes.

After some 10 days of operation, we noticed that the detector signals, before discrimination, were small at the beginning of each burst, increasing by around a factor of 4 in the second half of the spill. Attributing this effect to radiation damage of the sensors, we decided to profit from a MD period to replace the beam tracker modules with the second set of modules, which had never been exposed to the beam. It turned out that the module closest to the target did not provide any signal in one sensor and was very inefficient in the other. One of its original sensors had been damaged during the cryogenic test that followed the assembly of the cover. That sensor was replaced but the repaired module could not be tested afterwards since the electronics was already installed in the experiment. After the run, we saw that the new sensor had a high leakage current and found a grounding problem in the delivery of the bias voltage to both sensors. The second beam tracker station, at 30 cm from the target, operated well from the first moment, without any signal degradation from radiation damage, as expected of new sensors.

2.2 Operation in the October 2002 run

During the summer we assembled four microstrip modules to be used with heavy ion beams. Functionality tests were performed during the module production, after every assembly step, including a final source test with the amplifier and read-out system used in the beam area. After a few iterations in some of the assembly steps, all sensor channels of the four modules were properly operating. Two modules were installed in the cryostat and successfully operated during the 10-days run of October 2002, providing high quality signals in all channels. The corresponding bidimensional beam profiles are illustrated in Fig. 1.

During the first week of operation the cryogenic system worked very well, cooling down the modules to 130 K efficiently and keeping that temperature in a very stable

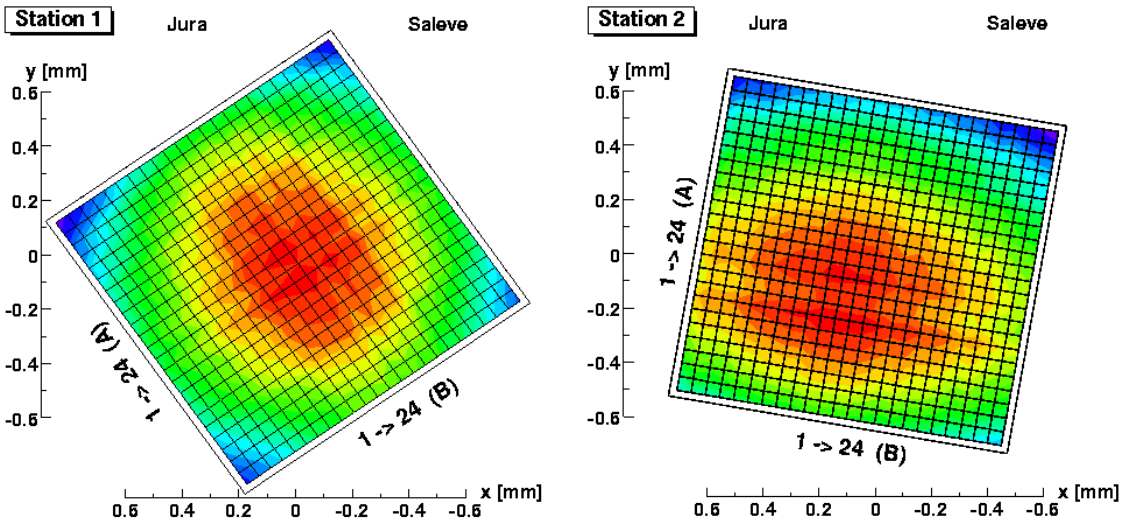

Figure 1: Beam profiles integrated over one burst by the upstream (left) and downstream (right) stations, during the 20 GeV/nucleon Pb beam time.

way. However, in the middle of the run the cryogenic system started behaving in a very unstable way, no longer keeping the modules cold for long periods. Frequent flow and pressure adjustments were needed to recover normal running conditions and, after some days, the coolant flow stopped being sufficient to provide enough cooling. This means that the beam tracker was basically running at room temperature during the last days of the run. Given the rather low radiation damage suffered by the detectors (we were running at very low beam intensities) and given the big signals deposited by the Pb ions, this was not a major problem for this run.

After discussions with colleagues from the Cryogenics Laboratory (LHC-ECR) and from RD39, the problem has been attributed to the presence of ice crystals in the liquid nitrogen, which usually sit at the bottom of the dewar and are not harmful to the operation of the detector. During the refilling operation the larger crystals may have been stirred up into the transfer line, clogging the narrow pipes running along the detector modules. Among other improvements, we will place a filter in the transfer line to prevent ice crystals from entering the system.

2.3 Performance of the Beam Tracker

The data recorded on tape shows that, during the proton run, the average horizontal beam position moved by around half a millimeter between the start and the end of the burst. A similar but less pronounced effect was observed with the wider low energy ion beam.

In the heavy-ion run, the beam tracker signals were very clean. The time spectra in all channels were basically noise free and peaked like delta functions, with the timing remaining within one bin (1.7 ns) throughout the run. At 20 V detector bias,

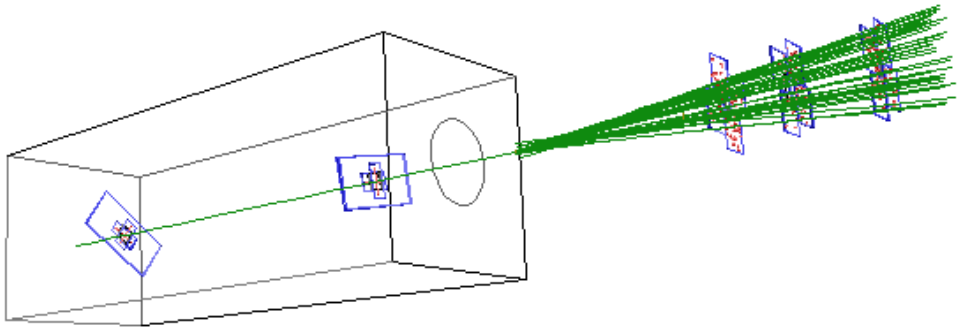

Figure 2: Trajectory of a 30 GeV/nucleon Pb ion reconstructed in the beam tracker. The particles produced in the target are tracked with the pixel planes.

the signals were around 1.5 V when running at 130 K and around 0.7 V when running at (almost) room temperature. Figure 2 shows the reconstructed trajectory of a beam ion, together with tracks seen in the pixel planes.

3 The Silicon Microstrip Telescope

3.1 Introductory remarks

Given the successive delays in the availability of the silicon pixel planes, and in order not to lose the proton beam time of year 2002, we decided, in March 2001, to proceed with the design and construction of a silicon microstrip telescope, to be used only in the proton runs. In taking this decision, we were very careful in making sure that only a very limited amount of resources would be focused on this new development, and in no way would there be negative interferences (in terms of human or financial resources) with the crucial development of the pixel detectors.

In fact, the silicon microstrip telescope had actually a few advantages with respect to the pixel telescope, previously expected to be used both with proton and ion beams. Indeed, the bigger sensor dimensions allowed us to place the last tracking station at 40 cm from the target centre, improving the momentum resolution thanks to the bigger $\int B\,\mathrm{d}L$ with respect to the pixel telescope, where the last plane was expected to be placed at around 26 cm, given the smaller geometrical coverage provided by the 16-chip pixel planes. Furthermore, the only material budget on the way of the particles we want to measure is the 300 μm thickness of each silicon sensor, since the readout electronics and corresponding cooling are outside of the tracking angular acceptance. In the case of the pixel planes we need to add the 750 μm thick readout chip and the hybrid support, besides the copper cooling circuitry just behind the chips. These two changes resulted in an improvement of the simulated dimuon mass resolution with respect to what was mentioned in the NA60 proposal, from $\sim$20 to $\sim$15 MeV at the ω mass.

Another important aspect that should be mentioned concerns the read-out speed. The ALICE1LHCB pixel readout chips run with a clock frequency of 10 MHz. Given the fact that, in a fixed target experiment, the trigger arrives asynchronously with respect to the read-out clock, and in order to ensure that all the hits from a given collision are stored on tape, in spite of the timing fluctuations among the 8000 pixel cells of each chip and among the different planes, we must use a strobe width of two clock cycles. This means that the maximum beam intensity we can run with is limited by the interaction pile-up occurring in a 200 ns time window. This is presently the limiting factor in the physics performance of the experiment when running with ion beams. We recall that when the NA60 proposal was written it was assumed that the pixel read-out chip would run at 40 MHz. The use of microstrip planes, which provide 25 ns analog sampling within the 100 ns surrounding the dimuon trigger, should allow us to identify and reject the pixel hits that are not in time with the collision that produced the dimuon. However, this will not work in the ion runs.

To finish these introductory remarks, we should underline that having a silicon microstrip vertex telescope working in June 2002 was very useful to develop, understand and commission many related issues, like the cooling system, the temperature monitoring, the (remotely controlled) CAEN power supplies, etc. Installing, debugging and operating a 16-plane telescope in the magnet gap was a good experience, in many down-to-earth aspects that could not be appreciated in laboratory tests. This learning curve was taken into account in the development of the pixel telescope, for instance improving mechanics and alignment items, and leading to the use of SMD Pt100 components placed on the pixel hybrids, for the measurement of the temperatures.

In summary, we can say that we have successfully developed and operated the new microstrip telescope, in spite of all the limitations (essentially in terms of time and expert human resources) and difficulties we experienced in facing this challenge. We should emphasize that this work would not had been possible without the excellent collaboration of the ATLAS SCT and of the EP-ED LHC-B teams, which developed, respectively, the readout chips and the ADC cards we used, among many other things. The high quality help of the EP-TA1 group (including the bonding laboratory) must also be mentioned here. The next sections provide more details on the assembly and operation of the microstrip telescope.

3.2 Detector and electronics assembly

A total of 16 silicon microstrip planes could be built and installed inside the PT7 magnet. Two other planes were prepared but could not be used in the beam, essentially because of the heavy workload of the bonding laboratory. The available planes were grouped back to back in 8 stations. Each plane contained 12 analog SCTA128VG radiation-hard read-out chips, in two hybrids, reading 12×128 strips at a clock frequency of 40 MHz. Upon reception of a trigger command, the SCTA chips output 4 consecutive values from the analog data buffer for all 128 strips. These

values are then used to reconstruct the analog pulse shape which determines the timing of and the charge deposited by the particles crossing the sensors. The sensor geometry (location, orientation, length and pitch of the 1536 strips) was designed to optimize angular and momentum resolution in our vertical dipole field, while keeping an approximately constant occupancy over the area of the sensor, in spite of the steeply changing angular distribution of the charged particles produced in a fixed target environment. The overall dimensions of the sensors were determined by the requirement of covering the angular acceptance window of the muon spectrometer at around 40 cm from the target, while fitting in the gap of the magnet. The complexity of the sensor geometry required a second metal layer to route the signals from the strips to the readout chips.

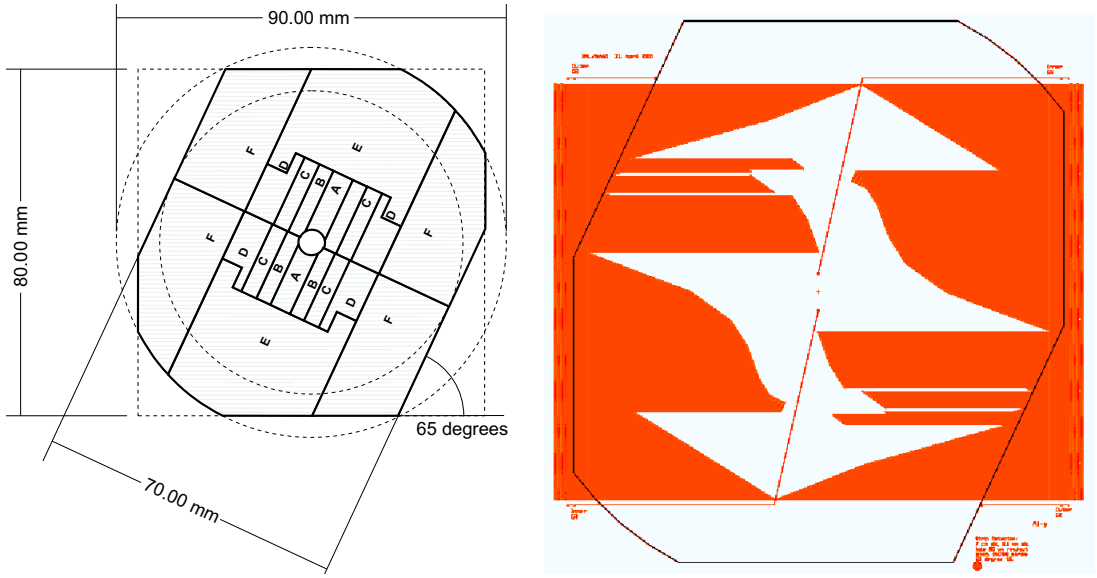

Figure 3: Geometry of the NA60 microstrip sensors: layout of the active strips (left) and readout lines mask (right).

Figure 3 shows the different areas of the sensor, characterized by a different strip pitch, between 60 and 227 μm, and the mask of the readout lines layer. The second metal layer is placed on top of a thin polyamide layer, resulting in an increased strip capacitance and contributing significantly to the noise of the detector. Figure 4 shows that the measured noise pattern can be reasonably described by the superposition of different terms basically corresponding to the areas of the active strips, of the readout lines and of their crossings.

When we started testing the sensors and assembling the modules, we found that many microstrip sensors had very high levels of 'leakage' current, which prevented proper biasing. After a lengthy debugging phase we realized that these currents resulted from a resistive contact between the back side of the silicon wafer and the end of the top most readout lines. The sensor mask was designed to cover the largest possible area within the 4 inch diameter wafers. While the active strips

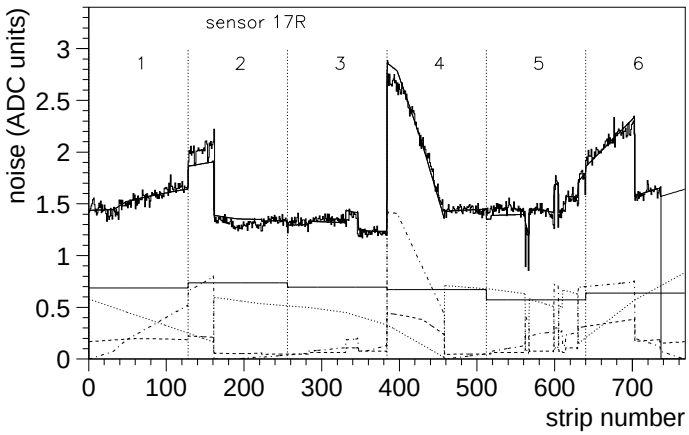

Figure 4: Comparison between the electronic noise pattern of a sensor, as a function of strip number, and the sum of the areas covered by the strips and corresponding read-out lines.

were always well within the silicon, in many sensors the readout lines that end up in a top corner of the sensor were too close to the physical edge of the wafer, due to a small misalignment during the metal deposition phase. Once the problem was understood, we cut the contacts between those extreme readout lines and the back side of the sensor, immediately decreasing the 'leakage' current from hundreds of μA to a fraction of a μA, in most of the sensors. Only one out of 18 sensors did not recover, and could not be used.

Also the development of the electronics chain used to configure, control and read out the microstrip telescope required a time consuming debugging phase. The central control boards, a crucial component for the control and synchronization of all 16 planes, were produced in the USA and could only be fully operated at CERN at the end of May, when the run was about to start. The commissioning of the new quad input mezzanines also took longer than expected. Given these unforeseen difficulties, the strip telescope could only be installed in the experiment at the end of the first week of run. Only then could we proceed with the final integration of this new telescope in the DAQ and control system of the experiment, and start the final debugging of the whole detector system.

The full readout electronics system, as installed in the experimental hall, was essentially composed of 4 PCs, equipped with SSPCI cards with quad-input mezzanines, reading 16 ADC cards, one per strip module, the whole system being controlled and synchronized by two central control boards. The low and high voltages were provided by two CAEN crates, remotely controlled via PVSS. Several modules had the cables directly soldered to their buffer cards, as can be seen in Fig. 5, since the thickness of the connectors would have prevented us from placing the modules as close to each other as needed. The quad-input mezzanines were connected to SSPCI SLink boards, that we upgraded so as to hold more than 5 average sized events in their buffer. This memory upgrade effectively decoupled the (asynchronous) PCI read-

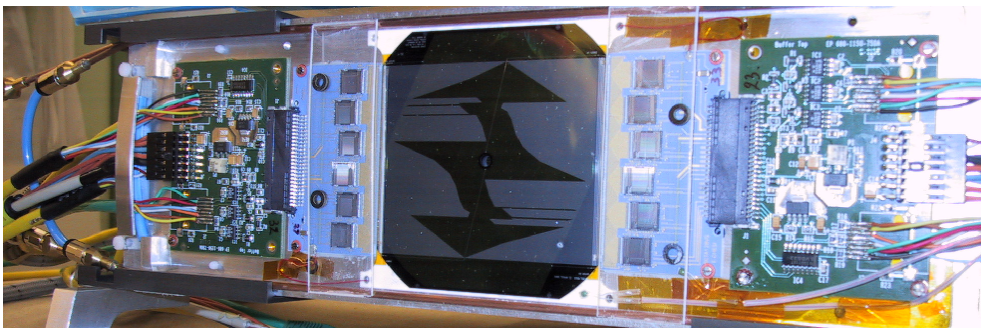

Figure 5: Strip plane installed in the last slot of the support box.

out from the (synchronous) front-end data push. To ensure correct operation, we decided to take the safeguard of dedicating a PC to each SSPCI+mezzanine group, even though a single PC could run the four boards. The system had two central control boards, for the synchronization and configuration of the SCTA chips and of the ADC cards. The latter was also the clock tree root and the interface with the trigger system. A JTAG router was implemented in order to access the JTAG ports of the individual components, the JTAG configuration being done via one parallel port. This scheme configured 192 SCTA chips and 16 ADC cards in a few seconds. The system was timed with a low intensity beam, both with a trigger provided by the Interaction Counter and with the dimuon trigger. A much more detailed description of the readout electronics system of the microstrip telescope can be found in Ref. [7].

3.3 Operation

The modules were connected to a cooling unit providing water at around 11–12 °C. The temperature of each module was measured in the hybrid and in the ceramic frame where the sensor was glued. At the beginning of the run (with current in the magnet) the measured temperatures were around 20–23 °C, when powering the chips. However, in the last week, due to a problem in the water cooling system of the PT7 magnet, the temperatures of the modules increased considerably, reaching values around 30–33 °C.

During the initial setting-up and debugging period several channels of one of the Central Control Boards stopped working and could not be quickly repaired. Therefore, most of the data were collected with only 14 sensors being read out. The pedestals and the noise associated to the different input channels of each chip have been analyzed for several data files collected along the beam time period, showing that the detectors performed in a stable way during the whole run. The only noticeable change in the noise was due to the cooling problem of the magnet.

In order to properly estimate the signals deposited by the particles, we must first subtract the ‘common mode’, electronic pick-up which usually appears as a coupling to the detector and to the electronic circuits of the read-out chip. In our case, it strongly depends on the capacitance of the strips, so that a linear determination

of this externally induced level must be performed for each of the regions of the sensor. Figure 6 shows the measured noise pattern, before and after common mode subtraction, showing how important it is to apply this correction to minimize the noise values. This is possible thanks to the availability of the analog information provided by the SCTA chips.

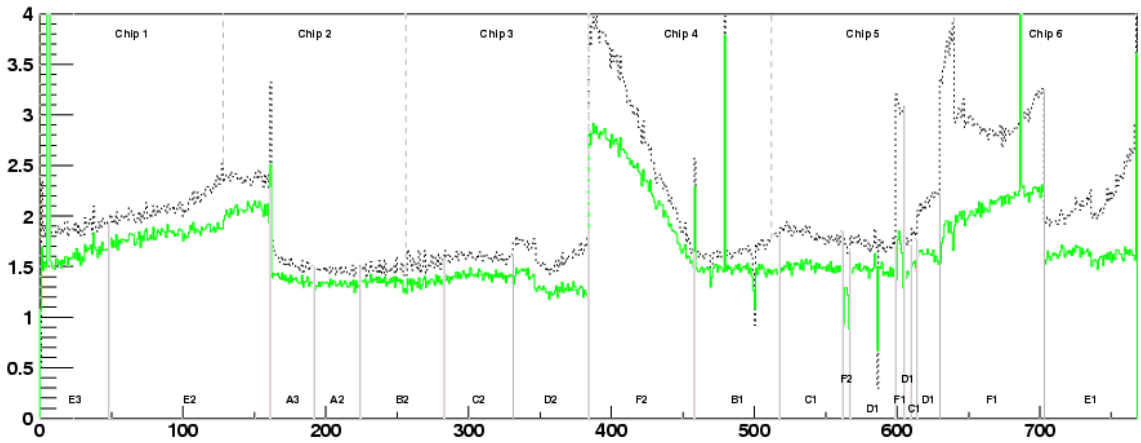

Figure 6: Electronic noise before (dotted line) and after (solid line) common mode correction, as a function of the channel number.

The ADC values of the four time samples are analyzed after subtracting their pedestal and correcting for the common mode. Strips previously selected by a broad criterium are fitted to a functional form of the pulse shape, as illustrated in Fig. 7. Two of the parameters describing this shape are specifically related to the electronic properties of the readout chip and are fixed from data collected with eight time samples, using calibration pulses. The other two parameters, the pulse height and

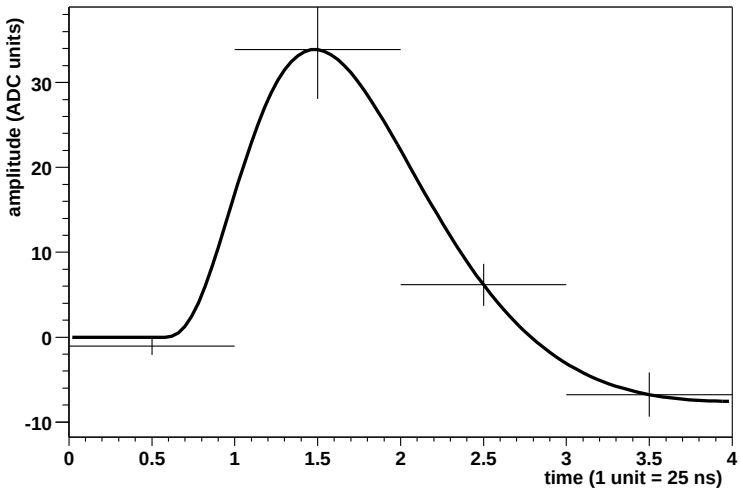

Figure 7: Fit of the four time samples, to extract the pulse delay and amplitude.

the pulse delay, are left free in the fit to our data.

Figure 8 shows the signal distribution obtained for a region with small strip pitch, before clusterization. The signal deposited on the strips was obtained by fitting the pulse shape, as described above. The measured pattern is properly described by the convolution of a Landau signal distribution with a Gaussian noise.

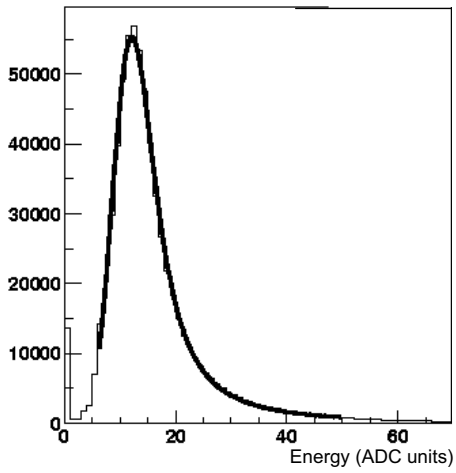

Figure 8: Measured signal distribution fitted with a smeared Landau function.

The data were collected with a bias voltage of 70 V. A quick voltage scan was performed between 70 and 100 V, in a few consecutive runs, showing that the lower value was enough to collect most of the deposited charge, with only a very slight increase when using 100 V.

4 The Silicon Pixel Telescope

4.1 Detector assembly

The NA60 silicon pixel telescope will consist of 16 planes, arranged along the beam axis as illustrated in Fig. 9. The nine planes closest to the target are made of four pixel chips, while six 8-chip planes constitute three large logical stations. Another 4-chip plane is placed just behind the first large station, to complement its beam hole and provide a better coverage of the muon spectrometer's angular acceptance. Located in the 2.5 T dipole field of the PT7 magnet, it will measure with good efficiency the angles and momenta of the charged particles produced at the target, even in the high multiplicity environment of high energy heavy ion collisions.

A single chip assembly consists of a 750 μm thick ALICE1LHCB pixel readout chip bump bonded to a 300 μm thick silicon sensor, having 8192 pixel cells, of 425×50 μm^2, arranged in a matrix of 32 columns by 256 rows. They are glued and wire bonded on two different ceramic hybrids, designed to hold either 4 or 8 chips. The small (4-chip) hybrids are mounted on two kinds of printed circuit boards, named

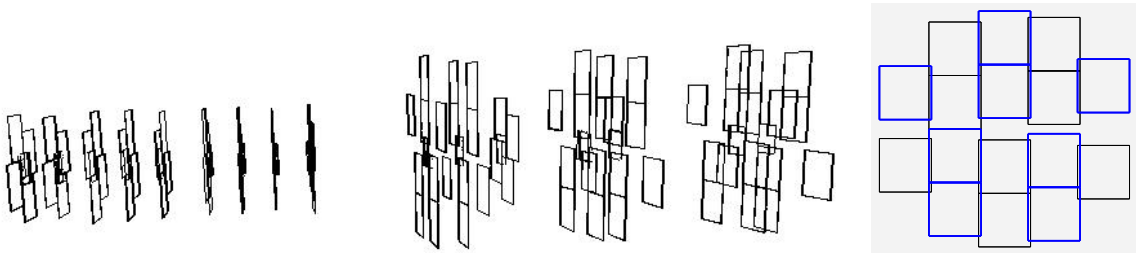

Figure 9: Global layout of the full silicon pixel telescope. The right panel shows the overlap of two 8-chip planes. In this plot, the Jura side is on the right.

X and Y, depending on the orientation of the 50 μm side of the pixel cells, while the 'large' planes are all of the X kind. The PCBs interface all signals with the data acquisition, control and power supply systems, and are mechanically supported by aluminium frames, that fit in a box placed in-between the magnet shims. All the signal cables exit from the 'Jura' side, while the 'Saleve' side is used to connect the planes with the cooling system. To optimize the overall acceptance coverage, some planes (named X' and Y') are inverted upside-down, having their back side facing the beam. The small planes are oriented according to the pattern X, Y, X', X', Y', X, X, Y, X' and X'. All the large planes are X−X' pairs, with the pixel detectors facing each other. Figure 10 shows the three 4-chip planes already produced and used in the October run. On the right side we see the back side of one plane, including the cooling ring and the copper pipe, where water at 15 °C circulates. To improve the cooling efficiency, the new 4-chip hybrids will be made of BeO instead of Al_2O_3.

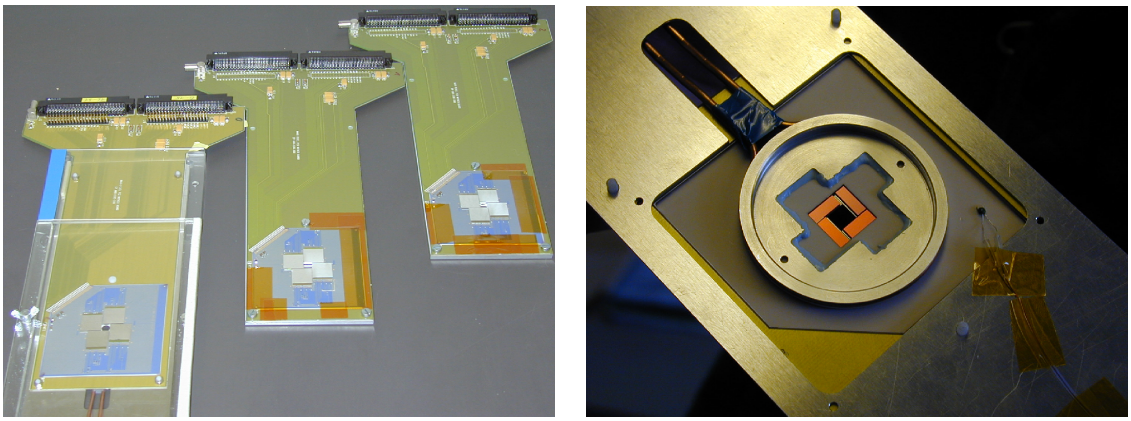

Figure 10: Photos of the 4-chip pixel planes used in the October 2002 run. The aluminium ring seen on the right panel houses a small cooling copper tube.

This telescope design minimizes the number of different components to produce: only two different hybrids and three different PCBs. The procurement of each of these components requires a lengthy procedure, starting with the design of the schematics and layout, continuing with the production of the pieces (including cutting to the

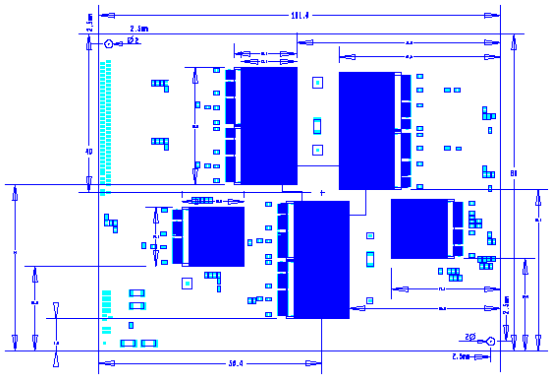

Figure 11: Layout of the 8-chip hybrid.

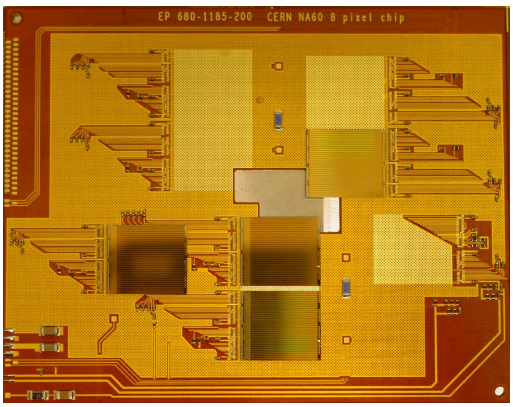

Figure 12: Prototype 8-chip hybrid, under test using readout pixel chips.

specified geometry) and their electrical tests, and finishing with their final commissioning, with several chip assemblies mounted and fully characterized in the laboratory. Of course, it is crucial to go through a prototype phase to fully debug the whole production chain. Figure 11 shows the layout of the 8-chip hybrid, while Fig. 12 shows a photograph of a prototype 8-chip hybrid, made of copper, being tested with readout pixel chips. The irregular beam hole minimizes the material budget close to the beam axis while ensuring a good heat dissipation of the inner chips. The final 8-chip hybrids are made of AlN substrates, which have a higher heat conductivity than the standard Al_2O_3 plates. Three such hybrids are now available and bump-bonded pixel assemblies will soon be mounted on one of them.

4.2 Status and prospects of the readout electronics chain

Each pixel cell contains a preamplifier, a shaper and a discriminator, as well as control and readout logic to transfer the binary hit information out of the chip. The discriminator threshold is set with a global voltage and then adjusted for every pixel individually with a 3-bit correction DAC. Furthermore, every pixel cell can be masked from readout or selected for test injections with an internal pulser.

The chips are read out at 10 MHz by a dedicated readout electronics chain based on the PCI bus. The system used during the October run was essentially the same as used in June, and a detailed description can be found in our previous memoranda [4]. Three readout chains were used, one for each plane, and the three PCI cards were plugged in a single PC. The configuration software and online monitoring were upgraded to handle multiple plane configurations. The main difference with respect to the June run was that the pixel planes were connected with the MB cards through 5 meter long cables. This allowed us to place the MB and adapter cards in a rack behind a concrete block, protected from radiation damage.

The use of this read-out system for the full telescope would still require, however, considerable changes in the cabling scheme on the side of the pixel planes, given the

high density of planes packed in the magnet gap. We are presently preparing an improved version, profiting from the pilot chip developed by the ALICE pixel project and from the 'GOL' chip. This improved system relies on an adapter card containing the two chips, called pilot adapter, and on a new PCI pilot mezzanine card. The pilot adapter is a small rectangular PCB plugged directly on a pixel plane. This has the advantage that the same pixel plane can be used either with the new or with the old version of the readout electronics chain without any change. In this way the testing is significantly easier: a direct comparison between the two readout versions becomes possible. Moreover, in case of failure of the pilot or GOL chips during run time, only the pilot adapter card must be replaced, without disturbing the detector plane.

The pilot adapter is interfaced to a pilot mezzanine card. The latter sends all pixel configuration commands to the pilot chip, which transmits them to the pixel chips (using the JTAG standard). Pixel data are transmitted by the GOL chip along a high speed serial line and received by the pilot mezzanine. This serial line replaces the bus connection implemented with large flat cables, allowing a considerable simplification in the mechanical aspects of the cabling. The pilot mezzanine is interfaced to the PCI-FLIC card, as in the readout scheme used in the 2002 runs. Presently two pilot adapter cards and two pilot mezzanines have been produced, and the testing of the new system is under way.

4.3 The October 2002 heavy ion run

The three four-chip pixel planes have been tested in detail before being installed in the experiment. For instance, Fig. 13 shows the measured threshold values versus the pixel number for a complete plane, yielding an average threshold of 2004 e^- with an overall r.m.s. width of 187 e^-. Since the noise was typically around 150–200 e^-, we could set the threshold to 2000 e^- during data taking.

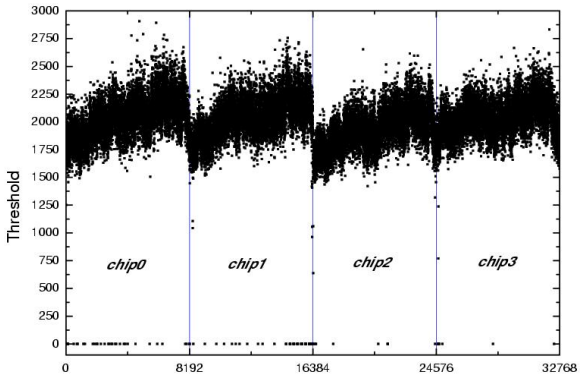

Figure 13: Threshold measurement, in electrons, of a full pixel plane.

The three planes were successfully operated during the Pb beam period. The hit-maps of all three planes (see Fig. 14 for an example) exhibit only very few noisy pixels (less than 0.1 %) and the dead pixel cells are in good agreement with what

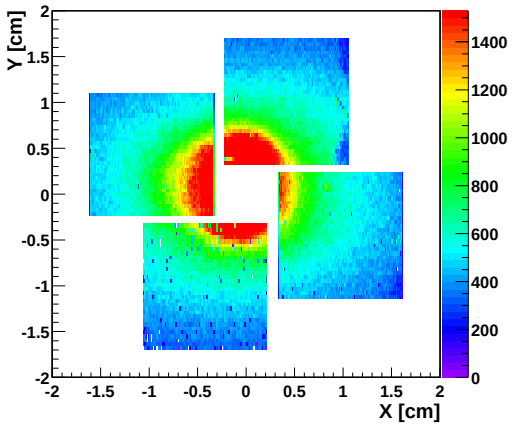

Figure 14: Hit-map of a pixel plane integrated over a few bursts in the October run.

was found in source measurements done on a probe station. The system worked well during all the run, allowing smooth data taking with a trigger rate of a few thousand triggers per burst. The temperatures measured behind the chips ranged between 20 and 25 °C. Special runs were frequently taken to monitor the detector behaviour. In particular, we regularly performed a threshold scan, by injecting a varying test charge into the pixels' preamplifier, to look for possible changes in the operation of the pixel chips. These tests showed no appreciable change during this short run period at low beam intensity.

We also periodically took special runs in which we varied the pixels' global discriminator threshold or the sensors' bias voltage, as illustrated by Fig. 15. These data

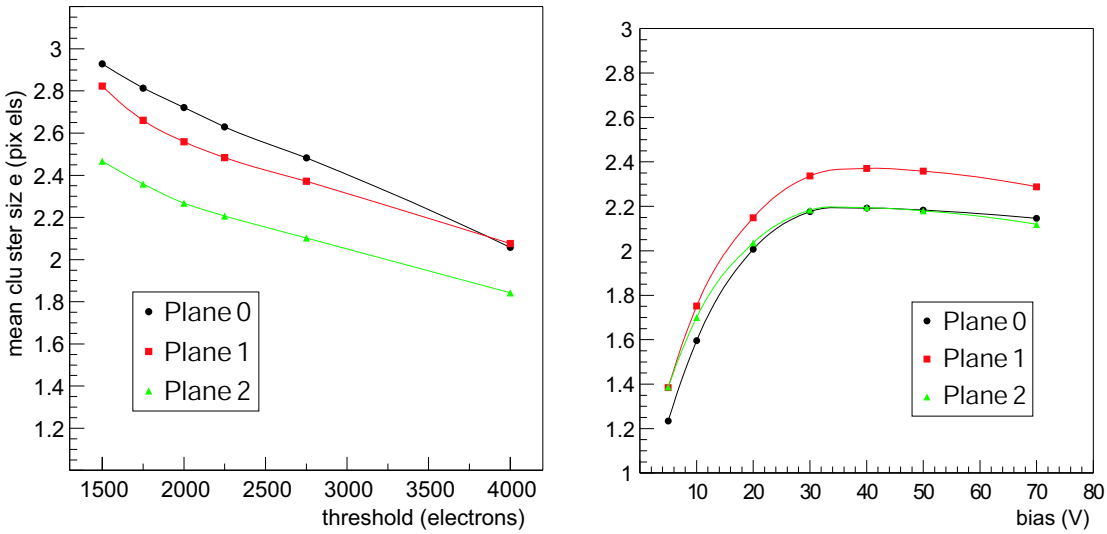

Figure 15: Average cluster size versus threshold (left) and detector bias voltage (right), for the three planes used in the October run.

show that the pixel detector behaved in the experimental setup just as it had during the laboratory tests. The nominal bias voltage of 70 V is safely on the plateau of full depletion. The dependence of the cluster size on the threshold gives us a means of controlling the charge sharing and thus the occupancy and spatial resolution without compromising the detector efficiency. Further analyses using the tracking information are ongoing.

Four columns of the ALICE1LHCB pixel readout chip (the so called test columns) have a slightly different electronic circuit design from the other 28. This difference gives rise to inefficiencies, which depend on the pixel cell and fluctuate significantly from one run to the next. Despite our efforts, this effect persisted both in laboratory measurements and in the June run. In the October run it disappeared from all the four chips of the 'old' plane that we had already used in the proton run, while the two new planes were affected. A systematic study is now in progress to understand how to control the behaviour of these test columns.

4.4 Results of the readout wafer tests

Four new wafers of ALICE1LHCB readout chips, with 86 chips each, have been tested on a probe station. For each chip the following tests were performed:

- Measurement of the analog and digital current consumption.
- Test of the JTAG functionality.
- Determination of the lowest threshold setting without noise hits.
- Measurement of threshold and noise for every pixel, and determination of the total number of dead and inefficient pixels.
- Characterization of the on-chip current and voltage DACs.

Wafer	Class 1	Class 2	Class 3
P8VM1GT	57	8	21
PRVM1YT	49	10	27
PSVM1XT	53	10	23
PVVM1UT	52	16	18
Total	211 (61 %)	44 (13 %)	89 (26 %)

Table 1: Chip quality summary of the four tested wafers.

The results of these tests classify the chips according to their quality (see Table 1). Class 1 chips are essentially perfect, while class 2 chips cannot be used in the experiment but are good enough for tests. A total of 211 class 1 chips were found, 2.4 times the number needed for the full pixel telescope, and 90 chips have less than 5 dead pixels (out of 8192). The average thresholds are typically around 15–20 mV, in good agreement with values measured on previously used chips. These four wafers, with their maps of good chips, have now been sent for bump-bonding with the sensor wafers.

5 The Interaction Counter

The Interaction Counter (IC) is made of two identical scintillators, IC1 and IC2, 16 cm wide, 10 cm high, and 10 mm thick, preceded by a 5 mm thick Pb sheet of the same dimensions, to increase the signal from charged particles by converting a fraction of the photons. It is placed 42 cm downstream of the target centre, after the last plane of the tracking telescope and just before the pre-absorber of the muon spectrometer. The un-scattered beam traverses its central hole, of 11 mm diameter. For each of the two scintillators, two wavelength shifting fibre bundles carry to an XP2020 phototube the light collected along the top and bottom edges.

The IC identifies hadronic interactions occurring in the target region essentially through the measurement of charged particles produced within its angular coverage, $2.75 < \eta < 5$. The field of the PT7 vertex magnet eliminates any contamination from delta rays produced by the beam crossing the targets and vacuum windows.

The Interaction Counter serves several purposes. Most importantly, it discards dimuon triggers due to interactions further downstream (in the ZDC or beam dump) and it tags events with pile-up interactions within nanoseconds of the dimuon trigger.

The discriminated pulses of the two counters, IC1 and IC2, and their coincidence (less sensitive to noise), are recorded in an 8-channel MultiHit Time Recorder (MHTR) module, with a 1.7 ns time binning. The double peak resolution is good enough to distinguish signals separated by at least 10 ns. The same MHTR module also stores the dimuon trigger signal and pulses from the ZDC, the Quartz Blade, and the back plane of one of the silicon detectors of the beam tracker. The strobe signal of the microstrip and pixel readout will be added when available. These signals allow us to make a detailed characterization of the event history before and after the dimuon trigger, particularly useful to identify events with pile-up data recorded during the 200 ns pixel strobe.

The un-discriminated amplitudes of the IC1 and IC2 signals are also recorded through 10 ADC channels, eight of them being devoted to the study of the line shape of the IC1 signal. This pulse is fanned out into 8 fast gates 10 ns wide and displaced by 5 ns with respect to each other. A non-standard pulse shape indicates short time interaction pile-up. The ADC information can also provide a rough estimate of the number of charged particles emitted in the collision.

The ADC read-out system was set up and tested during the ion run of October 2002, while the MHTR read-out had already been used in the June run. The same detectors were used in both data taking periods, simply changing the high voltages of the photomultipliers. The stability of the timing and amplitude spectra is checked online, both as a function of the run number and as a function of the time of the trigger within the burst.

6 The ZDC and the Quartz Blade detector

The Zero Degree Calorimeter (ZDC) measures the energy of the non-interacting 'spectator' nucleons, or beam fragments. It only works with nuclear beams and is removed from the beam line during the proton runs. During the Pb run of October 2002, even though the energies of the beam, 20 and 30 GeV/nucleon, were far away from the range where the response of this detector is optimal, the device has been successfully used, both to select (at the trigger level) events with interactions and to measure (offline) their centrality.

The trigger capabilities of the detector relied on the fast generation of the signals (based on the Cerenkov effect). Two different kinds of trigger signals have been implemented. The first one, the 'beam-trigger', is generated whenever the signal in the detector exceeds a certain minimum threshold. In this way we read out the detectors in coincidence with the arrival of an incident Pb ion, irrespective of having that ion interacting or not in the target region. The second kind of trigger, known as 'interaction-trigger', required that the collected signal does not exceed a threshold corresponding to $\sim$ 70 % of the maximum total incident energy (the 'lead peak'), thereby choosing events where a significant fraction of the beam energy has been deposited in the target region.

Figure 16 illustrates the ZDC energy spectrum obtained with the 30 GeV/nucleon incident Pb beam. The peak seen at $E_{\rm ZDC} \sim 6.2$ TeV is due to the non-interacting Pb ions, while the continuous spectrum at lower energies corresponds to events where the incident Pb ion interacted upstream of the ZDC. The histogram shows the events collected with the beam-trigger while the shaded area represents the events selected with the interaction-trigger, properly normalized. This figure shows how efficiently this signal selects events where an interaction has taken place.

As will be shown in the data analysis section, the ZDC information is used to divide the event sample in centrality classes corresponding to a certain range of impact parameter, b, or number of participant nucleons, $N_{\rm part}$.

The ZDC is complemented by a Quartz Blade detector (QB), positioned in front of the calorimeter, whose Cerenkov signal is proportional to the sum of the squares of the charges of the particles passing through (mostly nuclear fragments). During the October run we used two such detectors. The first one was made up by three pieces of crystal quartz, each one 15 cm long, glued together to form a 45 cm long slab. One extremity was positioned in front of the ZDC, while the other was read out by a Hamamatsu R5900U photomultiplier tube. In the second part of the run we used a second device, made of a 40 cm long single slab of amorphous silica (suprasil), read out by the same kind of photomultiplier. In Fig. 17 we show the two corresponding ADC spectra, taken with the beam-trigger. In both spectra we can see the peak corresponding to Pb ions crossing the QB, plus a continuum at lower ADC values, corresponding to events where the incident beam particle fragmented due to an interaction upstream of the QB. The squared charge of the Pb ions was measured with the crystal quartz blade with a resolution of 4.5 %, while the suprasil blade measurements

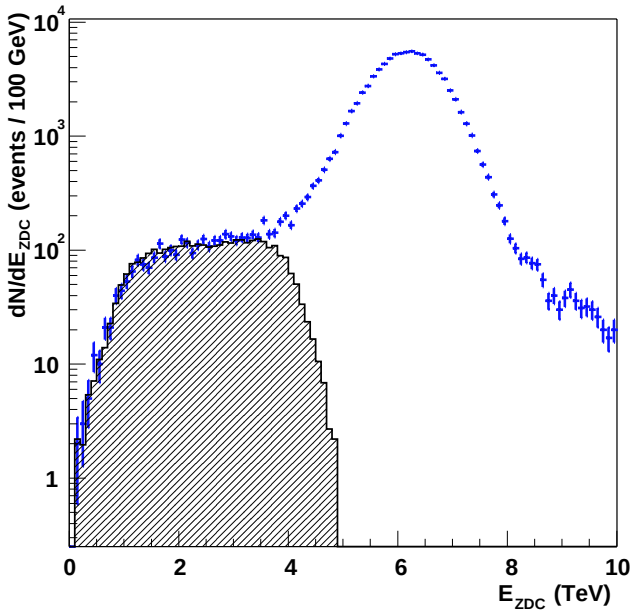

Figure 16: ZDC energy spectrum for the 30 GeV/nucleon incident Pb beam.

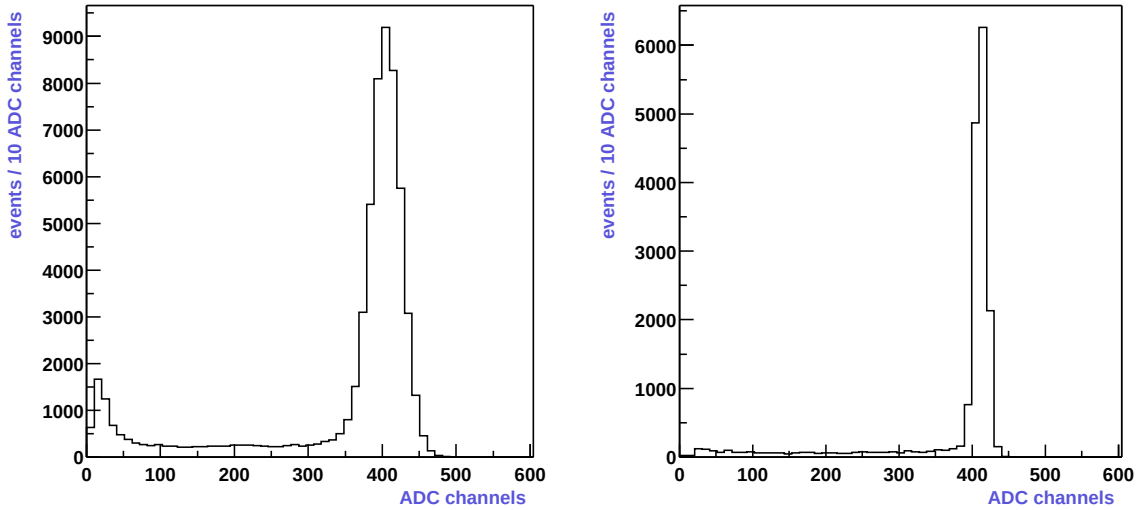

Figure 17: Quartz blade ADC spectra, corresponding to the 20 GeV/nucleon Pb beam, obtained with a threefold crystal quartz blade (left) and with a suprasil single blade (right).

exhibit a much better resolution, of the order of 2 %. This is probably due to the improved light transmission of the second device. The suprasil blade will be used in the forthcoming NA60 ion runs.

The QB detector is very useful to complement the ZDC information, in particular to reject events where no collision took place in the target, thanks to the good QB resolution in the region of the Pb peak.

7 The Muon Spectrometer

During the commissioning run of October 2001, the muon spectrometer was running without chamber 5, due to a gas leak, and without one of the three wire planes of chamber 6, because of a broken wire.

During the winter shutdown a considerable effort was devoted to the finding and repairing of all the gas leaks, even small ones, in all the chambers. In particular, chamber 5 could be operated without any noticeable gas leaks. Three broken wires were replaced in one of the wire planes of chamber number 6. After the repair and with the proper gas mixture, the chamber was then placed under high voltage, which was slowly increased up to the nominal value. After several hours of proper running, at least one wire must have broken again in the wire plane that had been repaired, the one that measures the 'V' coordinate. After a few days of running another wire broke, this time in chamber 5. Unfortunately, out of the three measuring wire planes (Y, U and V), this accident also occurred in the V plane. This means that the 'backward telescope', composed of chambers 5, 6, 7 and 8, could only provide two points for the V track projection. In these conditions, we can still do the tracking of the muons but we cannot calculate the efficiency of the backward chambers.

The repair of broken wires is a rather lengthy operation, requiring the availability of expert people, from CEA-Saclay, and of special equipment, to handle the (rather big) chambers, besides requiring access to the experimental hall for several consecutive weeks. The equipment we have used in the past, whenever was needed, is now in use by the Compass experiment, implying that new tools will have to be prepared. The combination of these external constraints with the time availability of our chamber experts, from Clermont-Ferrand, imposed that the broken wires of chambers 5 and 6 could not be repaired by the end of 2002. The work will be done in the first months of 2003.

During the October 2002 run, the muon chambers have not been operated, because the very low collision energy results in a very low dimuon acceptance within the rapidity coverage of our spectrometer. Besides, the very low production cross-sections and the very short beam time available would prevent us from gathering any relevant statistics for dimuon physics studies. We have only operated the trigger scintillator hodoscopes, to work on the programming of the trigger system and to commission a new read-out chain of the P2 mean timers, that provide a measurement of the time difference between the two muons that give the dimuon trigger. These two topics are mentioned in more detail in the next section.

8 Data Acquisition System and Trigger

The DAQ system of NA60 is based on PCI data acquisition boards (PCI-FLIC and SSPCI/SLINK) and Linux PCs running DATE-based DAQ software performing read-out and event building. CERN's central storage facility, CASTOR, is used for permanent data storage.

For the proton run in June 2002 a new detector, the Silicon Microstrip Telescope, was fully included into the overall DAQ. The readout chain consists of analog SCTA chips (near the sensor), buffer cards, ADC cards and two central control boards (CCB). The data is sent to SSPCI/SLINK boards, through appropriate input mezzanine cards, inside the LDC PCs. Since the SSPCI/SLINK cards work synchronously and do not have a spill buffering capability, a special SSPCI driver was developed to collect the data into the RAM buffer (in the PC) during the spill. There were four LDCs, each containing one SSPCI/SLINK card which read up to four ADCs. The configuration of the front-end electronics was performed by a separate LabVIEW program (using a software JTAG controller via the parallel port) to allow experts more flexibility. The direct configuration from DATE was also tested. A new monitoring package, based on the NA60 monitoring framework, was prepared and operated.

During the June run we have also tested the first 4-chip pixel plane. We used the so-called MB card setup with the FLIC/PRB and a special adapter card in-between. JTAG configuration was performed through the FLIC using a purely software controller, with a special program that read the parameters from a MySQL database and was called by DATE at the beginning of each run. The partition was operated as a stand-alone LDC during the initial test period and was later successfully integrated in the overall DAQ, running routinely together with its monitoring package.

The new readout of the Beam Tracker was commissioned. It consists of a FLIC card with a FERA mezzanine (same hardware as the RMH mezzanine but with a specifc FPGA design to handle the FERA protocol) that reads out the FERA bus connecting the MHTR and ADC modules. This avoids using a FERA memory, which has a very limited capacity and requires a slow CAMAC-GPIB interface with the PC, incompatible with trigger rates of several thousand per burst.

During the proton run, a multiple event-builder configuration was used, with up to 3 GDCs. Such a system will be needed when the experiment will run with high data rates (about 150 MB/burst). After the initial debugging period, the DAQ as a whole (up to the permanent data storage) performed well, with some 100 GB of data stored on tapes.

Concerning the trigger, a new system was developed to make the OR of the BUSY signals coming from each DAQ partition. Only once all the partitions had cleared their BUSY signal, the trigger system was allowed to take another event. The system incorporates a TimeOut feature so that the trigger system is released after a certain time, even if one of the partitions gets blocked. The number of time outs per burst is counted by a CAMAC scaler, which is read at the end of the burst. During the normal data taking period this counter remained always at zero. In case such a timeout error happens, we can examine the error words provided by the FLICs to see in which event and in which partition the problem occurred.

For the October 2002 low energy Pb run the pixel part of the DAQ was modified to handle several FLIC cards in one LDC PC. The JTAG configuration program and the monitoring package were modified accordingly. The three pixel planes started running in a stand-alone mode for setting-up and tests, and were afterwards added

to the overall DAQ.

The new ZDC readout has also been fully commissioned and routinely operated. It uses the same technology as the Beam Tracker, i.e. a FLIC with a FERA mezzanine reading LeCroy FERA ADCs (one CAMAC crate) and a GPIB link to CAMAC for configuration. It uses its own LDC and newly developed monitoring software, with the functionality of the Fortran code previously used in NA50.

A new FERA system, consisting of CAMAC TQC and FERA ADC modules, was built for the timing measurements done using the mean timers of the P2 hodoscope. This partition is merged with the ZDC, sharing the same CAMAC crate, FLIC card, FERA mezzanine and LDC. The corresponding monitoring software was also developed.

During this run, data were routinely collected with the beam tracker, the three pixel planes, the interaction counter, the quartz blade and the ZDC, using a standalone ZDC trigger that bypassed the standard electronics chain but which was timed with respect to the normal dimuon trigger.

In parallel, we performed a special study of the trigger programming, interfacing the logic unit specially built by NA10 to either the old NA50 DAQ (Fortran programs, running on a Vax and on a Motorola front-end processor) or to the newly developed C-based codes, running on the Linux DAQ PCs. Although time consuming, the comparison of the CAMAC 'dumps' for each trigger setting command, with the old and the new system, revealed some differences that could be understood and corrected. As a result, some anomalies observed in June in the trigger hodoscopes illuminations, when using the dimuon trigger, have now been eliminated. We should note that the programming of this complex and crucial 'Magic Box' CAMAC module, built 'in house' some 23 years ago, is not trivial to understand and could not be tested without beam time.

9 Detector Control System

The NA60 Detector Control System (DCS) provides control and monitoring of the cooling and gas systems, through PLCs, and of the power supplies, through CAENET and CAEN OPC servers. The PVSS and BridgeVIEW software packages centralize, archive and display the DCS data. Two Windows2000 PCs in the control room provide the user interface for the shift takers.

15 CAEN SY403 crates located in the control room provide the high voltages needed for the photo-tubes of the trigger hodoscopes, of the ZDC/QB and of the Interaction Counter. In the beam area, two SY1527 CAEN crates provide the high and low voltages needed by the silicon detectors (the Beam Tracker, the Silicon Microstrip Telescope and the Silicon Pixel Telescope) to bias the sensors and power the electronics. These crates are interfaced with the high-level software through CAEN OPC servers, either via CAENET (SY403) or Ethernet (SY1527).

A Wago PLC is used for the automatic regulation of the cryogenic system of

the Beam Tracker, depending on the temperatures measured on the detectors, using Pt100 Wago modules. The same devices provide temperature monitoring for the Strip and Pixel Telescopes. A Schneider PLC controls the gas flow in the muon tracking chambers. It is interfaced with PVSS or Bridgeview through a Schneider OPC Server running on a Windows PC. In case of need, the DAQ PCs located in the beam area can be reset from the counting room, using the PVSS user interface to command interlock relays, through the Wago system.

The top-level SCADA application was developed using PVSS software, communicating with the hardware via the OPC servers. PVSS panels were developed for all the equipments using the JCOP framework, developed by the CERN IT/CO group. A main panel shows the most important parameters of the experiment, and gives access to more detailed views of specific sub-systems in devoted panels. The time evolution of the most important DCS values is permanently on display using a Bridgeview application. These values are also regularly exported to an external archiving system, based on MySQL, and can be viewed from any web browser through a CGI Perl script. Such history browsing can be very useful during the offline data analysis.

In general, we can say that our PVSS-based Detector Control System worked quite smoothly during the October 2002 ion run, with less problems than during the June 2002 proton run. Several pragmatical solutions were implemented (resets, automatic restarts, fully devoted PCs, etc) to minimize the frequency and importance of the problems. For the next run, some further changes need to be implemented on the software (e.g., new panels for the pixel telescope), on the hardware (new SY1527 cards) and on the interfacing (CAEN OPC Server instead of SLIC-DIM to control the SY403 crates). We are confident that our Detector Control System has now reached a mature level and we do not foresee any major future difficulties.

10 Offline Software

The offline software of the NA60 experiment, called na60root, is a multipurpose package based on ROOT: an object-oriented framework developed at CERN. It consists of several sub-packages used for Monte-Carlo simulation, raw data reading and decoding, data reconstruction, and detectors alignment and calibration. It started from the framework developed by the ALICE offline team, AliRoot, but then developed rather independently, becoming fully devoted to the specific needs of NA60.

The detector response simulation package consists of two parts. The generation of the collision is performed by one of the external event generators, such as the widely used Pythia, Venus and URQMD Monte-Carlo generators, or by private generators used to reproduce kinematical distributions according to empirical functions. Then the generated event is given to the na60root tracker which, using GEANT 3.2111, propagates the particles through the detector and performs digitization. In the end it produces the output file in the same format as the decoded experimental data. One can superimpose several events, either produced by the same generator to simulate

interaction pile-up, or by different codes to obtain an event with a triggered dimuon from a hard process (using Pythia) embedded in a heavy-ion collision (generated by Venus).

The simulation of the background muon pairs from pion and kaon decays is still under development, and includes a fast simulation option to speed up the time consuming running of the GEANT package. In this option the pions and kaons are forced to decay in all the generated events, and the program keeps track of the appropriate decay probabilities.

The raw data reading package consists of separate modules for each type of detector and allows a fast decoding of either the whole event or of some specific branch of data. The version of the DATE package which we are using to store the raw data does not allow us to read data from multiple streams. This is a problem for NA60, since the data of a given run can be split between two or three GDCs (Global Data Collectors). Some effort has been invested on developing a solution to this drawback and a new I/O system, developed as a stand-alone package, is now being tested and incorporated into na60root.

The data analysis package allows track reconstruction in each individual detector and matching between different detectors. An improved version of the muon spectrometer reconstruction code is now working without problems. We have verified that the efficiencies of the chambers extracted by the new algorithm are similar to the values observed during the NA50 experiment.

The track reconstruction in the Silicon Vertex Telescope allows track finding in setups including both pixel and strip detectors (as well as only one kind). It still needs some improvements to speed up the analysis in the case of mixed telescopes (used in proton runs) and to decrease the fraction of fake tracks. It is being used to reconstruct the data collected in 2002, with quite reasonable results. The matching between the muon tracks and the tracks in the Vertex Telescope is already available but some fine tuning still needs to be done.

The algorithm for determining the interaction vertex using the tracks in the vertex telescope has been developed and successfully tested both with p-A and Pb-Pb data. It is capable of reconstructing multiple vertices in events with interaction pile-up. The resolutions obtained from Monte-Carlo simulations for the determination of the interaction vertex, in p-A and in Pb-Pb collisions, are in good agreement with what we observe in the real data. More details are given in the next section.

The package for the Beam Tracker data analysis allows track reconstruction either with both stations or with only one. The latter feature was used for the reconstruction of the June 2002 p-A data, when the downstream station did not work. In this case the resolution of the position of the beam particle at the target is determined by the beam divergence. Nevertheless, we still see a good correlation between the beam track and the reconstructed interaction vertex.

Apart from the improvements mentioned before, considerable work is needed on some important sub-packages of na60root. For instance, for the moment the dimuon background subtraction is done only at the Muon Spectrometer level, with the method

used in NA50. It accounts only for the combinatorial background originating from uncorrelated decays of pions and kaons. The use of this method requires applying an additional cut to the data, ensuring that the acceptance of a muon with given kinematics does not depend on its charge. Such a cut decreases the signal statistics by up to a factor 2 in the ρ/ω mass region and shrinks the accessible phase space window. To avoid such losses we will use the 'mixed events' technique, building the combinatorial background sample from muons randomly picked from different events. A preliminary version of this algorithm was written in Fortran a long time ago, but still has to be improved and added to na60root.

Another major issue is the subtraction of the background due to the fake matches between the tracks in the Vertex Telescope and the muons from the Muon Spectrometer. Presently we have no data requiring such procedure, since in the p-A data the number of tracks in the Vertex Telescope is not high enough to create such background and the Muon Spectrometer was not running in the low energy Pb run. The corresponding package will be ready in time for the heavy-ion run of 2003.

In summary, while much work still needs to be done, we can say that the NA60 offline software has now reached a mature status, and is able to perform most of the tasks needed for the simulation of the experiment and for the reconstruction of the collected data. We are now doing the analysis of the p-A data taken in June 2002 and of the Pb-Pb data taken in October 2002. A first report on the progress of that effort is given in the next section.

11 First results from the 2002 runs

11.1 Analysis of the June p-A data

As already mentioned above, most of the June 2002 proton beam period was devoted to the setting-up and commissioning of the new detectors. In particular, the microstrip telescope was only fully operational in the last week of beam, a week devoted to collect data for offline analysis, with both polarities of the ACM and PT7 magnetic fields. The data was collected at beam intensities between 2 and 5×10^8 protons per burst, lower than what we had anticipated, to ensure that we could use the information of the interaction counter and of the single working station of the beam tracker. Furthermore, being the first time we were using the strip telescope for tracking, and knowing that our sensors had relatively high levels of noise, we preferred to work with low levels of pile-up.

Given the short beam time available and the beam intensities used, we have only collected around half a million dimuon triggers. Furthermore, in some data files (corresponding to around half of the events) we cannot use the information corresponding to one or two tracking planes. In particular, after a few days of operation, one of the sensors developed too much leakage current, preventing proper biasing during the last collected 'runs'.

The algorithm for determining the interaction vertex using the tracks in the vertex

telescope was developed and successfully tested with the June data. It is capable of reconstructing multiple vertices in events with interaction pile-up. The measured Z-vertex distribution, shown in Fig. 18, clearly reveals the presence of each of the six sub-targets. Taking into account the 2 mm thickness of each target, we extract from this distribution a Z-vertex resolution of ~ 900 μm. This is in good agreement with what we expected, from Monte-Carlo simulations, for the resolution of the vertex determination in the low multiplicity p-A interactions: 30–40 μm in the transverse (X and Y) coordinates and around 900 μm in the Z (beam) direction.

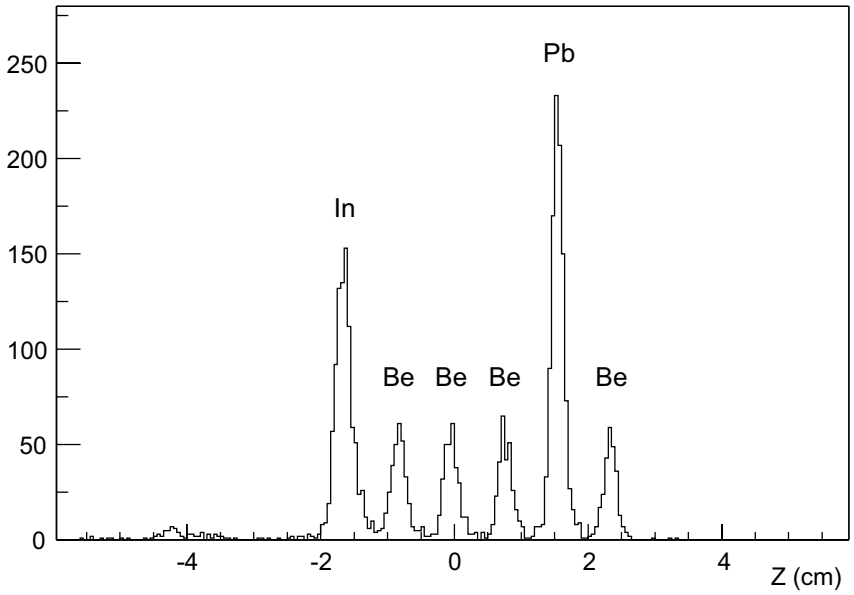

Figure 18: Z-vertex distribution measured by the microstrip telescope during the June p-A run, showing the different targets used.

As mentioned above, during the second part of the June run only one station of the beam tracker was working, the one most distant from the target system, and we had to modify the reconstruction algorithm to work in these conditions. This means that the resolution on the measurement of the transverse position of the incoming beam particle on the target becomes dominated by the divergence of the beam. Assuming a beam divergence of around 0.5 mrad, the extrapolation to the target of the proton flight path, measured in the station located 30 cm upstream, should have a resolution of around 150 μm. The observed difference between the transverse coordinates of the interaction vertex, obtained using the tracks measured in the vertex telescope or extracted from the beam tracker information, has a width around 150 μm, as expected if it is completely dominated by the beam tracker precision.

The track and vertex reconstruction is done using the information provided by all the working strip planes and by the 4-chip pixel plane, also installed in the telescope, and which was operational during several days. The telescope box had 19 'slots', the number nine being occupied by the pixel plane. The positions 10, 11, 14 and 15 were

not used: two of them were empty and the other two had strip planes that could not be read out. The strip sensor in position 12 was not fully depleted and only half of the strips of the sensors in positions 13 and 17 were read out. This means that, even though 14 strip planes were recorded on tape, only 11 can be considered as 'fully working'. Furthermore, the 4-chip pixel plane was essentially used for testing purposes and, to ensure easy access, was placed too far away from the targets, only covering around 75 % of the tracking angular acceptance. Figure 19 shows, for each of the 19 telescope positions, the working efficiencies of each plane, convoluted by their geometrical acceptances. We observe that the strip planes between positions 3 and 16 see around 85 % of the tracks produced within the angular acceptance of the muon spectrometer. The first two and the last two strip planes do not completely cover the acceptance window, respectively because the tracks go through the beam hole or pass outside of the outer edge of the sensors.

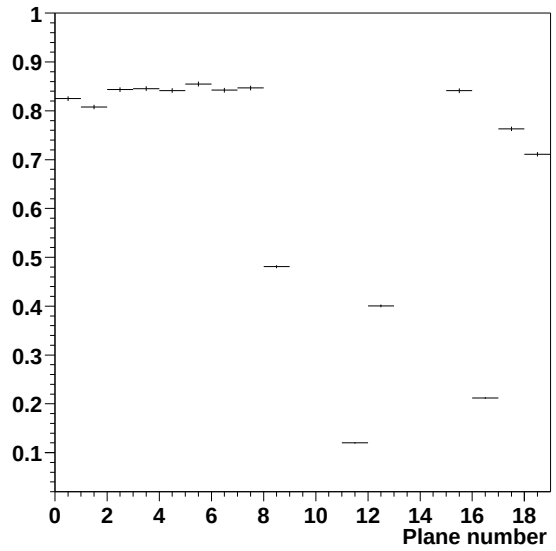

Figure 19: Efficiencies times geometrical acceptances as a function of the physical position of each tracking plane.

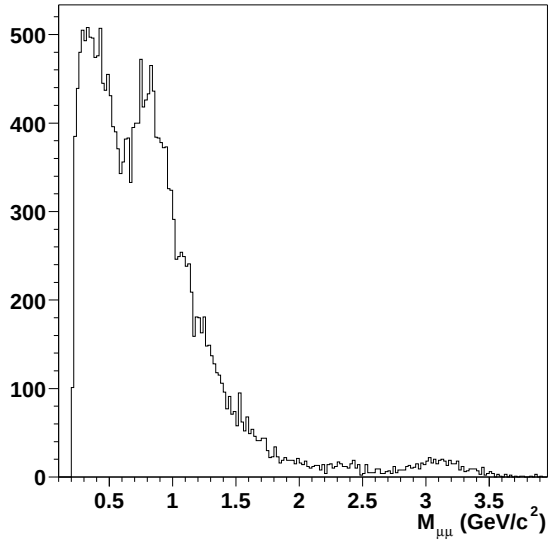

Figure 20: Dimuon mass distribution as directly measured by the muon spectrometer.

Figure 20 shows the dimuon mass distribution measured by the muon spectrometer, before using any information from the target region. It integrates dimuons produced in any of the six sub-targets or in any other material on the way of the proton beam. Since the total target thickness is less than 5 % of an interaction length, most of the beam interacts in the beam dump, surely producing many dimuons, some of them giving a trigger. A very preliminary estimate indicates that only $\sim$40–50 % of the dimuon triggers correspond to collisions upstream of the silicon tracking telescope. These numbers will be revised in the near future, once certain quality cuts are applied to the muon tracks (as previously done in NA50).

A first use of the silicon tracking telescope in the context of dimuon physics

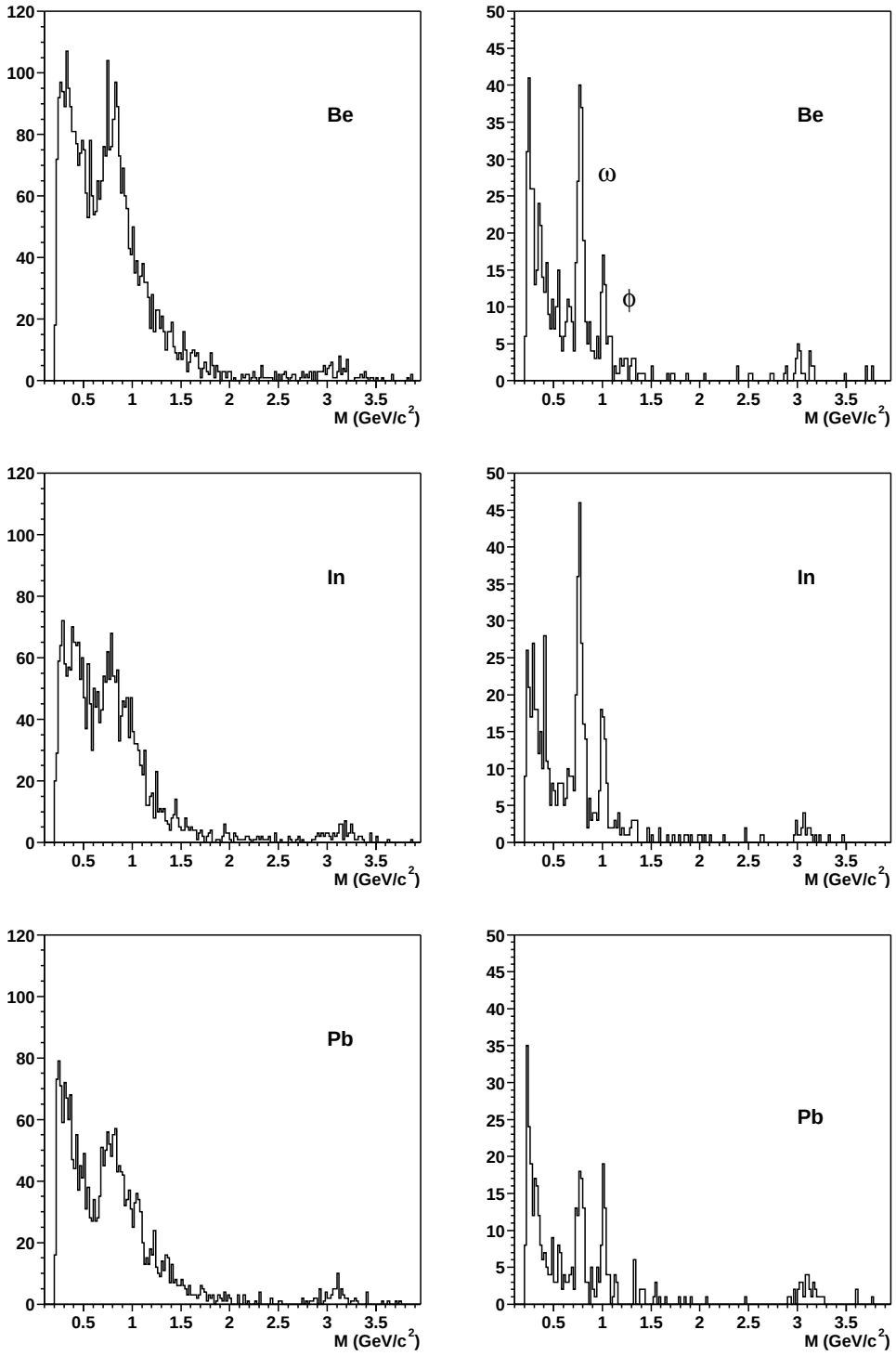

Figure 21: Dimuon mass distributions before (left) and after (right) doing the track matching between the muon chambers and the vertex telescope. Each row corresponds to a different target nucleus: Be (top), In (middle), and Pb (bottom).

consists in identifying the target where the interaction took place, so that we can sub-divide the dimuon events in p-Be, p-In and p-Pb sub-samples. This only requires reconstructing the Z-vertex of the collision, irrespective of finding or not the muon track in the silicon sensors. The left side plots of Fig. 21 show the opposite-sign dimuon mass distributions, as reconstructed by the muon spectrometer, for each of the three different target nuclei. The second (and much more challenging) use of the silicon tracking telescope is, of course, the matching of each muon track to one of the tracks reconstructed in the vertex telescope, immersed in the PT7 dipole field. Clearly, not all the events survive the muon track matching step. For instance, the fraction of opposite-sign dimuon events due to decays of pions or kaons decreases from $\sim 25\,\%$ to around $\sim 5\,\%$, because when the meson decays within or after the vertex telescope it gives a bad χ^2 for the track matching. The right side plots of Fig. 21 show the dimuon mass distributions of the events where the track matching procedure was successful. The improvement in mass resolution is obvious. These plots correspond to around $10\,\%$ of the collected statistics.

Only counting the events with the dimuon produced in the target, our present (very preliminary) estimate for the average single muon track matching efficiency is around $49\,\%$, leading to a dimuon matching efficiency of around $23\,\%$.

We emphasize that all the results presented in this section correspond to a preliminary phase of the whole data analysis effort, and much work is ongoing.

11.2 Analysis of the October Pb-Pb data

During the 10-day long October run, the NA60 experiment collected around 7 million Pb-Pb collisions at 30 GeV/nucleon and three times as many at 20 GeV/nucleon, with various set-up configurations and trigger signals. We can use these data samples to test, with the three pixel planes available, the tracking capability of the vertex telescope in ion-ion collisions. In fact, the charged particle multiplicity of the low energy Pb-Pb collisions studied during this run is similar to the one expected for In-In collisions at full SPS energy. Therefore, the tracking performance obtained by analysing the October 2002 data should provide a lower limit on the accuracy that will be reached in 2003, when the full vertex telescope will be available.

The three pixel planes were placed in the telescope box positions closest to the targets, so as to cover as much as possible an angular acceptance close to mid-rapidity. Note that, at these low energies, mid-rapidity sits one unit of rapidity backward with respect to the high energy interactions the experiment was designed for. As an interesting by-product of this test run, we can measure the charged particle rapidity densities within the covered angular range, for several ranges in the centrality of the Pb-Pb collisions, as estimated by the forward energy deposited in the ZDC.

The first step in the analysis of the October data consisted in the tuning of the track reconstruction and vertexing algorithms, in the accurate determination of all the alignment parameters, of the beam tracker and of the pixel telescope, and in the calibration of the ZDC and QB detectors. A first extensive reconstruction of the

collected data was then performed, during December.

The results obtained so far, even though still preliminary, are already good enough to demonstrate that all the detectors we used performed very well. As an illustration of the quality of the data, we show in Fig. 22 the reconstructed Z-vertex distribution, i.e. the distribution along the beam axis of the vertices wherefrom the measured tracks originate. This figure was done with data collected with the 30 GeV/nucleon beam. We can easily recognize three narrow peaks, corresponding to the three Pb targets used, complemented by a smaller peak, at $Z \sim -4$ cm, due to interactions in the window separating the beam tracker cryostat from the target box. The three Pb targets were placed at 2.4 cm from each other, along the beam line. Their thickness was 1.5, 1.0 and 0.5 mm, from the most upstream to the most downstream, all of them being 10 mm in diameter. The measured distribution can be described by convoluting the thickness of the targets with a Z-vertex resolution of around 200 μm.

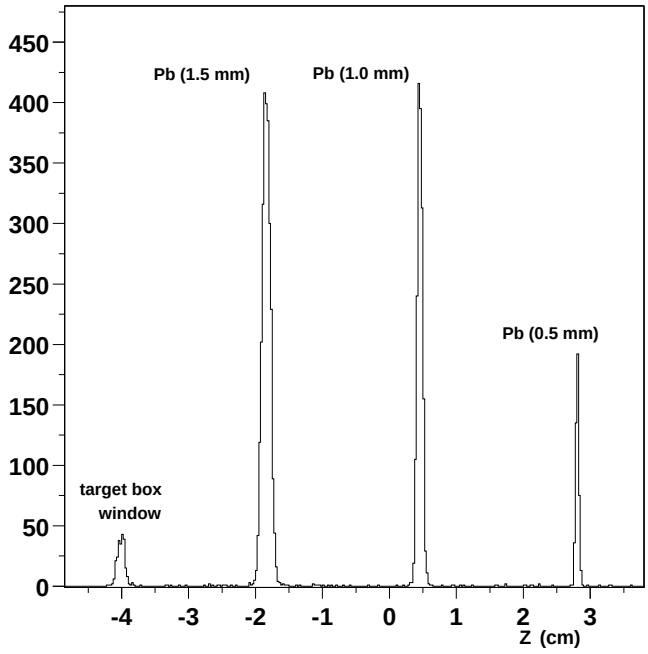

Figure 22: Z-vertex distribution, as determined by the pixel telescope, only selecting vertices with at least ten tracks.

We can evaluate the quality of the vertex reconstruction in the transverse plane by comparing the transverse coordinates of the incident beam particle, as reconstructed by the beam tracker, with the corresponding values calculated with the pixel telescope information. Figure 23 shows the correlation between the values obtained by the beam tracker and by the pixel telescope for the X-vertex (left) and for the Y-vertex (right) coordinates. The width of the correlations gives $\sigma_X \sim 30$ μm, in the direction of the smallest pixel cell side, and $\sigma_Y \sim 70$ μm, in the vertical direction. Taking into account the resolution of the beam tracker, we can deduce that the pixel telescope identifies the X-vertex value with an accuracy of around 20 μm. The resolution in

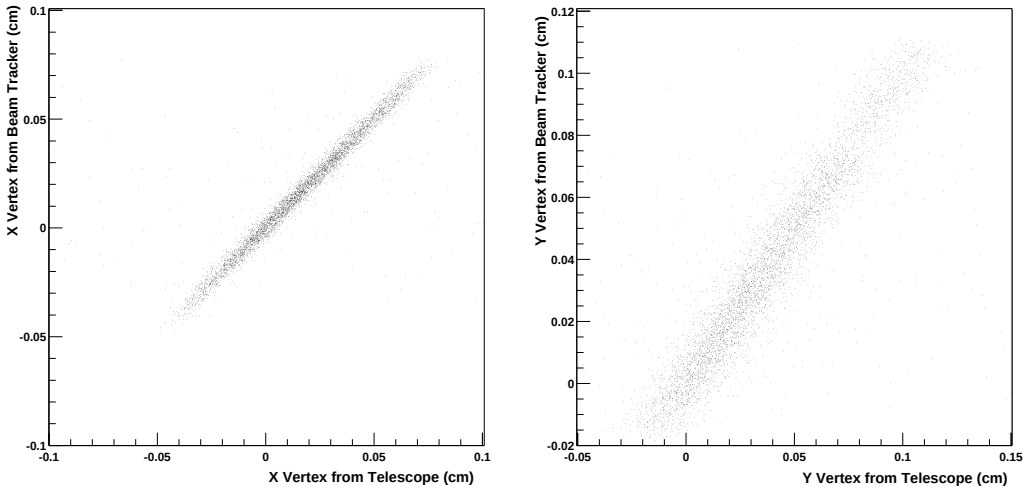

Figure 23: Correlation between the vertex position measured by the beam tracker and by the pixel telescope, for the X and Y coordinates.

the Y coordinate is not as good because all the three 4-chip pixel planes we used are of the X kind.

These results confirm that, in the dimuon physics runs of 2003, we will be able to identify the interaction point of the nuclear collision with very good accuracy. It is important to have a good measurement of the impact parameter of the muon track, to select events where two muons result from the decays of open charm mesons.

The centrality of the Pb-Pb collisions is inferred from the forward energy deposited in the ZDC. Figure 24 shows the $E_{\rm ZDC}$ distribution measured with the 30 GeV/nucleon Pb beam, as collected with the 'beam trigger'. The superimposed line represents the fit to a Glauber calculation, done in the range 0–4000 GeV. The extrapolation of the fitted curve into the peripheral collisions region, $E_{\rm ZDC} > 4000$ GeV, stops reproducing the measured points because the data becomes heavily contaminated by events where the incoming Pb ion has not interacted. Using the information provided by the Interaction Counter and Quartz Blade detectors, we can identify the region of the $E_{\rm ZDC}$ distribution due to Pb-Pb interactions in the target. We can divide that region in four event classes, of different centrality, as shown in Fig. 24.

If we slice the measured $E_{\rm ZDC}$ distribution at the values 1500, 2500, 3500 and 4500 GeV, for instance, we get four event classes that have certain probability distributions in terms of impact parameter of the collisions, shown in Fig. 25. Naturally, there is some overlap between the $\mathrm{d}N/\mathrm{d}b$ curves corresponding to neighbouring event classes, essentially due to the resolution of our $E_{\rm ZDC}$ measurement. Nevertheless, we can see that each event class has a well defined average impact parameter, showing that we can sub-divide our events, even at these rather small collision energies, in four well defined centrality classes, of significantly different collision geometry.

As an example of the studies we are currently performing, using the information provided by all the detectors operating in October, we show in Fig. 26 the anti-

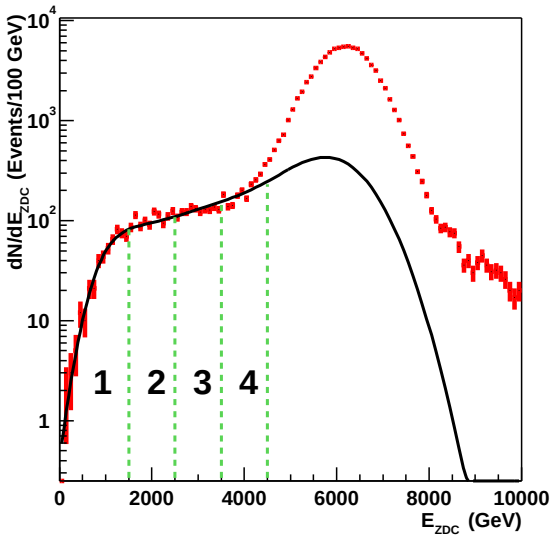

Figure 24: E_{ZDC} distribution measured for the 30 GeV/nucleon Pb beam, compared to a Glauber model calculation.

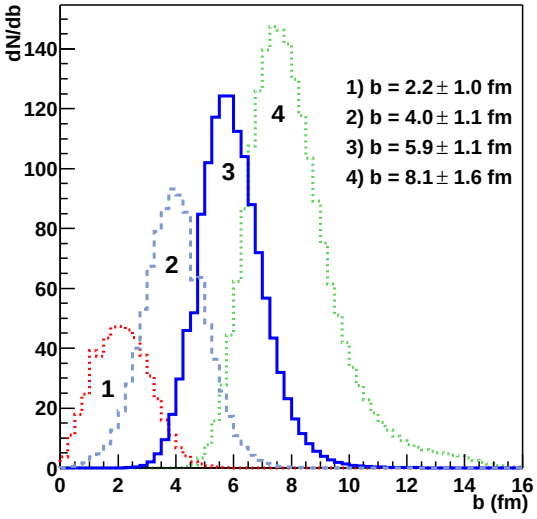

Figure 25: Impact parameter distribution of the events corresponding to the four centrality classes.

correlation between the number of reconstructed clusters in the most downstream pixel plane and the energy deposited in the ZDC. This particular plot was done with the data collected with 30 GeV/nucleon Pb ions. Of course, the more central collisions result in less beam spectators (low E_{ZDC} values) and in a higher multiplicity of produced charged particles (high number of clusters in the pixel planes).

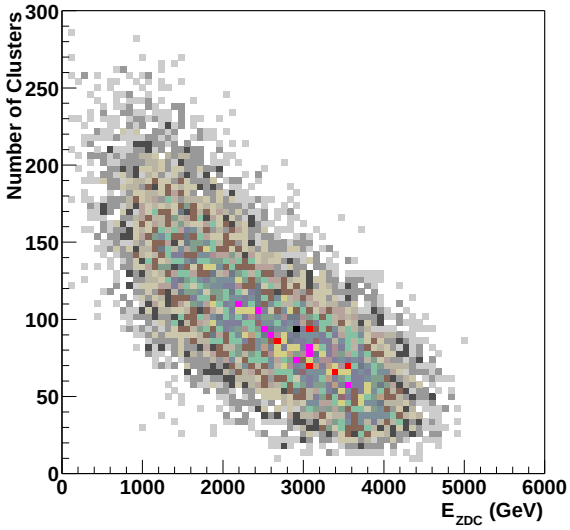

Figure 26: Correlation between the measured cluster multiplicity in the most downstream pixel plane and the energy deposited in the ZDC.

Some of the clusters seen in the pixel planes are due to background sources rather than to the charged particles produced in the Pb-Pb collisions. This contamination is essentially due to particles produced in secondary interactions (mostly by pions colliding in the surrounding materials) and to δ-rays created by the passage of the ion beam in the targets and in the target box exit window. We are currently studying these background sources. Once they are fully understood, and corrected for, we will overlap the angular ranges covered by the three pixel planes with respect to collisions taking place in each of the three targets, to extract the charged particles pseudo-rapidity density, $\mathrm{d}N/\mathrm{d}\eta$, in the forward hemisphere.

12 Prospects for the next runs

In 2003 the NA60 experiment will collect In-In collisions at 158 GeV per incident nucleon and p-A collisions at 400 GeV. The physics motivation and the anticipated detector performance for these runs has been explained in detail in the proposal of the experiment. The most important studies to be done with the heavy-ion data concern the measurement of the suppression pattern of the J/ψ and ψ' charmonium states, the measurement of the yield of open charm production, the search for the production of thermal dimuons, and the study of the production of the low mass vector mesons, ρ, ω and ϕ. These studies must be done as a function of the centrality of the In-In collision, and the results must be compared with the previous results from the study of Pb-Pb collisions (at the same energy) and with the reference baseline established from p-A data. In what concerns the proton-nucleus data, the main physics goals are the measurement of the nuclear dependence of the χ_c production, through the comparison of the ratio of production cross-sections χ_c/ψ in p-Be, p-In and p-Pb, and the measurement of the nuclear dependence of open charm production, using the same nuclear targets.

With respect to the proposal [1], the experiment has undergone several changes, in the target system, in the configuration of the vertex telescope, in the magnitude of the magnetic field, in the thickness of the pixel readout chips, etc. Therefore, we are presently redoing the simulations of the physics performance of the experiment. In particular, the increased thickness of the pixel readout chips and of the hybrids will lead to increased multiple scattering, particularly unfortunate for the planes closest to the targets. On the other hand, the stronger dipole field, and the extended tracking distance, will lead to an improved measurement of the tracks' momenta.

The physics performance for heavy ion runs will surely be affected by the slower operation clock of the read-out pixel chips. With 5×10^7 In ions per burst going through our multiple In target, and using a read-out strobe of 200 ns, around 50 % of the collected events will suffer from interaction pile-up, and should, in principle, be rejected. With a couple of tracking planes running at 40 MHz we would be able to select only the hits in a time window of 50 ns around the collision that gave the dimuon trigger, therefore recovering the events with pile-up. In practice, this would

be equivalent to extending the effective beam time by almost 50 %. Upgrading our pixel telescope in this way is an option for the future, if pixel detectors running at 40 MHz become available soon.

Important changes have also happened in the p-A setup, with respect to the text given in the proposal. Figure 27 shows the configuration of the silicon tracking telescope we are currently using to simulate the physics performance of the experiment for the next proton runs. It is a mixed setup, with eight strip stations complemented by six 4-chip and four 8-chip pixel planes.

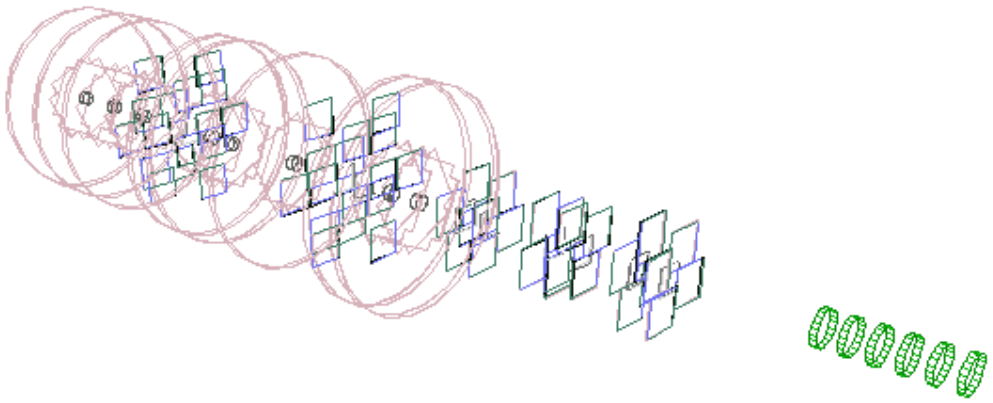

Figure 27: Vertex tracking telescope used in the simulations of the future proton runs.

The target system is the one already used in 2002, with the In target followed by three Be, one Pb and another Be targets, all of 2 mm thickness. The dimuons produced in the last Be target will not suffer from the multiple scattering and energy loss induced by the Pb target. We should recall that having all the targets simultaneously on the beam line eliminates the uncertainty on the overall luminosity normalization from the systematic errors of our most important measurements. Indeed, to extract the nuclear dependence of production cross-sections we only need to know the relative factors between the production yields from the different nuclear targets (corrected for acceptances, etc), and not the absolute production cross-sections for each independent target.

13 Summary and Conclusions

After the very successful heavy-ion test run of October 2002, we can say that the NA60 experiment has reached a mature level and we are confident that we will collect good data for dimuon physics studies in the next proton and ion runs. The technical feasibility of the most challenging project of the experiment, the silicon pixel telescope, has been demonstrated. However, the time schedule remains short and the

resources are limited. The next lines describe the steps being done to complete the pixel telescope.

During the last year, four read-out chip wafers were tested on a probe station and 211 chips were accepted as class 1, i.e. with less than 100 dead pixel cells out of 8192, from which 90 chips have less than 5 dead channels ($\sim 0.06\,\%$). On 17 December 2002 five sensor wafers were received from Canberra, each wafer containing 38 sensors, 300 μm thick. These wafers, together with the read-out chip wafers, were already sent to VTT, where sensors from 3 wafers will be bump-bonded during January and February to read-out chips of class 1, resulting in the best case in 114 pixel detector assemblies. Upon arrival at CERN these assemblies will be certified on a probe station using test pulses and a radioactive source. This test will last approximately 2.5 weeks for all assemblies. In case we do not reach immediately the 88 chips required, a second bonding process with sensors from the fourth wafer will be performed.

The PCBs for the 4-chip pixel planes, 10 X and 6 Y, including spares, are ready. The BeO hybrids for these planes will be produced soon and will be available by the end of February. We will then proceed immediately with the production of the 4-chip pixel planes. Assuming that the 8-chip pixel plane prototype is successfully tested around middle of January, the production of the AlN hybrids and the corresponding PCBs will be started. We expect all this material to be ready by middle of March. Around the same date the pilot chip PCBs should also be ready, assuming that the ongoing prototype tests are soon successfully concluded. During January the TA1 group will start the production of the aluminium frames and cooling sets; all the parts should be finished by middle of March. Remains the production of the support box for all the tracking planes, which should be ready in April.

In summary, we are working in view of having the pixel telescope ready before the summer, and we hope that we can collect enough data to perform a good study of our exciting menu of dimuon physics, both with proton and with high-energy ion beams.

Acknowledgements

We would like to express our gratitude to the many people that have contributed to the preparation of the NA60 experiment. A special word of thanks goes to the CERN groups EP-ED, EP-MIC, EP-TA1, EST-DEM, IT-CO, and LHC-ECR, for their help with the development of our electronics, detectors, gas systems, mechanics, controls, cryogenics, etc. The SL-EA group has been extremely helpful with the setting up and operation of our beam line and magnets. We are particularly indebted to the ALICE Silicon Pixel Detector team for all their help in what concerns the development, testing and operation of the pixel detectors. They surely contributed in a crucial way to the successful operation of our pixel planes in the June and October runs. We are also grateful to the ATLAS SCT and LHC-B VELO teams for their friendly collaboration in the construction of our microstrip telescope.

References

[1] NA60 Coll., "Study of prompt dimuon and charm production with proton and heavy ion beams at the SPS", CERN/SPSC 2000-010, March 2000.

[2] W. Snoeys *et al.*, Nucl. Instr. Meth. Phys. Res. **A465** (2001), 176;
K. Wyllie *et al.*, "A pixel readout chip for tracking at ALICE and particle identification at LHCb", Proc. of the Fifth Workshop on Electronics for LHC Experiments, Snowmass, Colorado, 1999.

[3] NA60 Coll., "NA60 Status Report", CERN/SPSC 2001-009, SPSC/M662, March 2001; CERN/SPSC 2002-009, SPSC/M679, March 2002.

[4] NA60 Coll., "Status Report on the NA60 Pixel Detector Project", CERN/SPSC 2002-024, SPSC/M689, May 2002; CERN/SPSC 2002-025, SPSC/M690, July 2002.

[5] V. Granata *et al.*, "Cryogenic technology for tracking detectors", Nucl. Instr. Meth. Phys. Res. **A461** (2001) 197;
RD39 Coll., "RD39 Status Report", CERN/LHCC 2002-004, February 2002.

[6] K. Borer *et al.*, "Charge collection efficiency of irradiated silicon detectors operated at cryogenic temperatures", Nucl. Instr. Meth. Phys. Res. **A440** (2000) 5.

[7] A. David, "The NA60 microstrip telescope readout electronics", presented at the 4th International Workshop on Radiation Detectors, Amsterdam, The Netherlands, September 2002.